AD NUMBER

ADB076818

NEW LIMITATION CHANGE

TO

Approved for public release, distribution unlimited

FROM

Distribution authorized to U.S. Gov't. agencies only; Test and Evaluation; 30 SEP 1993. Other requests shall be referred to Naval Ocean Research and Development Activity, Stennis Space Center, MS.

AUTHORITY

NSTL per DTIC form 55, 20 Aug 1993

(12)

NORDA Technical Note 219

Naval Ocean Research and Development Activity
NSTL, Mississippi 39529

Environmental Support for High Frequency Acoustic Measurements at NOSC Oceanographic Tower, 26 April - 7 May 1982; Part I: Sediment Geoacoustic Properties

Michael D. Richardson
David K. Young
Ocean Science and Technology Laboratory
Oceanography Division

Richard I. Ray
Computer Sciences Corporation
NSTL, Mississippi 39529

June 1983

EXECUTIVE SUMMARY

This is the first of a four-volume report on environmental support for a joint University of Texas Applied Research Laboratory (UT-ARL)-Naval Ocean Research and Development Activity (NORDA) high frequency acoustic experiment. The experiment was conducted near the Naval Ocean Systems Center (NOSC) Oceanographic Tower, one mile off the California coast near San Diego, California, from 26 April to 7 May 1982. The objective was to provide improved shallow-water acoustic models required for development of advanced mine-hunting sonar systems. In this report we present sediment geoacoustic measurements made concurrently with backscatter measurements for the NOSC Tower Experiment.

Two sediment types were evident from visual (scuba) observation and from laboratory analysis of sediment geoacoustic properties. The sediments closest to the transmit-receive tripod were coarse sands with higher compressional wave velocity and lower attenuation and impedance values than those of fine sands surrounding the target spheres.

Geoacoustic Property	Sediment Type: Coarse Sand	Sediment Type: Fine Sand
Mean Grain Size (Ø)	0.96	3.53
Velocity Ratio	1.15	1.10
Attenuation (k)	0.29	0.47
Compressional Wave Velocity (m/sec) @ 15°C, 34 ppt, 18m	1730	1655
Sediment Impedance (g/cm^2 sec $\cdot 10^5$) @ 15°C, 34 ppt, 18m	0.322	0.366

The variability of geoacoustic properties was slightly less for the coarse sand than for the fine sand and considerably less than reported for silty clay by Richardson et al. (1983).

Sediment compressional wave velocity and attenuation increased with depth in the sediment, probably as a result of a decrease in porosity due to compaction and packing. The differences between measured and predicted sediment acoustic properties can be explained by these gradients in geoacoustic properties. Historical data from near the NOSC Oceanographic Tower support these conclusions.

These surficial gradients in sediment geoacoustic properties may be important factors in the prediction of high frequency bottom reverberation.

ACKNOWLEDGMENTS

The authors particularly thank Matt Milligan, Computer Sciences Corporation, for logistics support at the NOSC Oceanographic Tower; and James Steward, Scripps Institution of Oceanography, for scuba operations logistics support. We also thank the Naval Ocean Systems Command Center for providing use of the Oceanographic Tower. Roxanne Mauffray typed the manuscript. This work was supported by NAVSEA Program Element 62759N, Edward D. Chaika (FY82) and Robert L. Martin (FY83) Program Managers.

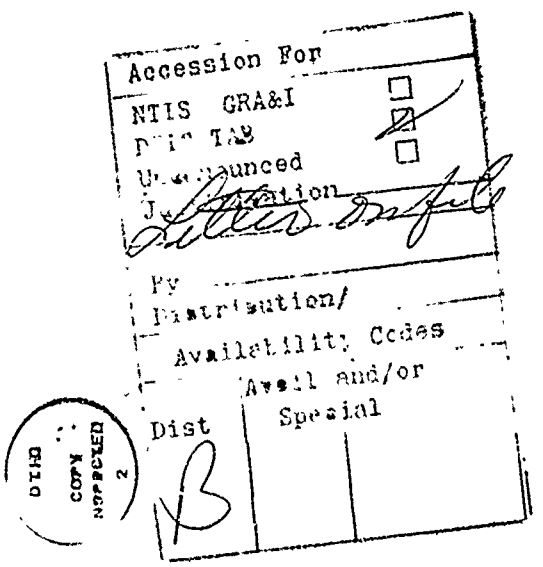

CONTENTS

ILLUSTRATIONS

TABLES

ENVIRONMENTAL SUPPORT FOR HIGH FREQUENCY ACOUSTIC MEASUREMENTS AT NOSC OCEANOGRAPHIC TOWER, 26 APRIL - 7 MAY 1982

I. INTRODUCTION

This is one part of a report covering environmental support for a joint University of Texas, Applied Research Laboratory (ARL-UT) and Naval Ocean Research and Development Activity (NORDA) high frequency acoustic experiment. The experiment was conducted near the Naval Ocean Systems Center (NOSC) Oceanographic Tower, off the California coast near San Diego, California, from 26 April to 7 May 1982. Participants from NORDA included David K. Young, (Code 334), Michael D. Richardson (Code 334), Steve Stanic (Code 343), Peter Fleischer (Code 361) and Roy I. Burke (Code 361). Participants from ARL-UT included T. G. Goldsberry, R. A. Lamb and S. P. Pitt.

The objective of this program is to provide improved shallow water acoustic models and databases for development of advanced mine-hunting sonar systems. At this time, system developers do not have reliable Environmental Acoustic (EVA) models or shallow water databases necessary for weapon system trade-off studies.

Effectiveness of mine-hunting sonar is limited by reverberation, primarily from bottom backscatter and secondarily from surface backscatter (Boehme et al., 1980; NORDA, 1982; NSWC, 1982). It is, therefore, imperative that AMSS system developers have models which predict the mean, range and variability of bottom backscattering coefficients for shallow water areas in which the AMSS will operate. These backscattering models must be applicable to low grazing angles (1-10°) in order to provide adequate standoff range for detection; include 30-95 kHz frequency range for both detection and classification of targets; and cover narrow beamwidths (1-3°), bandwidths (1-4 kHz) and wide range of

pulse lengths (0.15-25.0 m/sec) for utilization by AMSS and similar systems.

Bottom backscatter models have traditionally employed empirical regression models in predicting scattering coefficients for different grazing angles, frequencies and substrate types (McKinney and Anderson, 1964; Bunchuk and Zhitkovskii, 1981). Theoretical models have not been used to predict scattering coefficients because it is not known which scattering process is dominant at different frequencies, grazing angles, patch sizes of insonified areas or substrate types (Crisp et al., 1980). Both types of models require oceanographic parameters as inputs. Inputs include sediment compressional wave velocity and attenuation, sediment density, bottom roughness spectrum, bottom slope, and distribution of surface and volume scatters. These parameters are often empirically predicted from sediment mean grain distribution or porosity.

The next generation of MCM sonars as well as the AMSS will incorporate computer-aided detection techniques that require estimates of the spatial distribution, including means and variances of backscatter coefficients for meaningful performance prediction. Meaningful prediction of backscatter coefficients, therefore, requires concurrent measurement of the spatial distribution of sediment properties and bottom roughness characteristics as well as backscatter coefficients.

In this report, we present sediment geoacoustic measurements made concurrently with backscatter measurements for the NOSC Tower Experiment. These included the spatial distribution of sediment compressional wave velocity and attenuation as well as sediment grain size distribution. Part II includes data on sediment bottom roughness; Part III includes remote bottom characterization of the site and Part IV includes overall discussion, conclusions and recommendations for future experiments.

The acoustic backscatter data will be reported by T. G. Goldsberry, R. A. Lamb and S. P. Pitt in an ARL-UT Technical Report.

II. MATERIALS AND METHODS

A. DESCRIPTION OF STUDY SITE

Experiments were conducted at a site adjacent to the NOSC Oceanographic Tower, one mile off Mission Beach, California, (Fig. 1). Water depth was 18 m and the substrate type was medium to fine sand. A transmit projector and hydrophone receiving array were located 4.27 m above the bottom on a tripod tower approximately 200 m NW of the Oceanographic Tower (Fig. 2). This tripod was connected to electronic hardware on the NOSC tower by an underwater cable. Three aluminum target spheres filled with carbon tetrachloride and freon gas were placed on PVC pipe stands 75 m, 110 m, and 210 m away from the tripod tower.

During reconnaissance diving (scuba) we found two distinct substrate types in the experimental area. The tripod was surrounded by a coarse sand characterized by sand waves with 50-60 cm wavelengths and 10-20 cm heights. The target spheres were located in fine sand characterized by sand ripples with 10-20 cm wavelengths and 5 cm heights.

B. FIELD COLLECTION

All samples were collected with the aid of scuba (Table 1). Sediment samples were collected with cylindrical cores during six dives. Each cylindrical core was 45 cm long and bevelled at one end to improve penetration. Cores were capped at both ends immediately after collection to retain the water overlying the sediment and kept in an upright position during transport. Two cores were collected at each target sphere site (cores 1-6); four

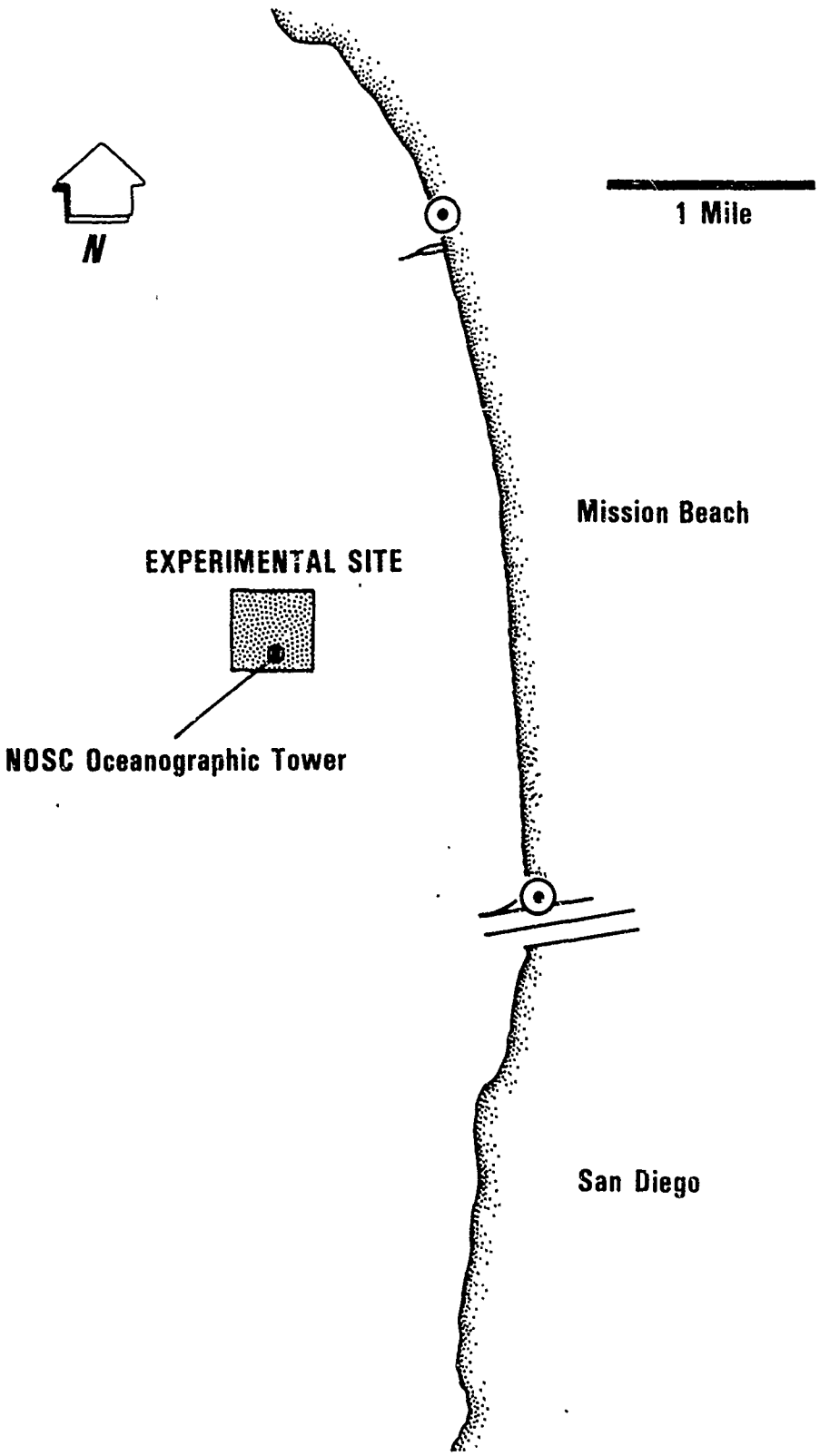

Figure 1. Location of experimental site.

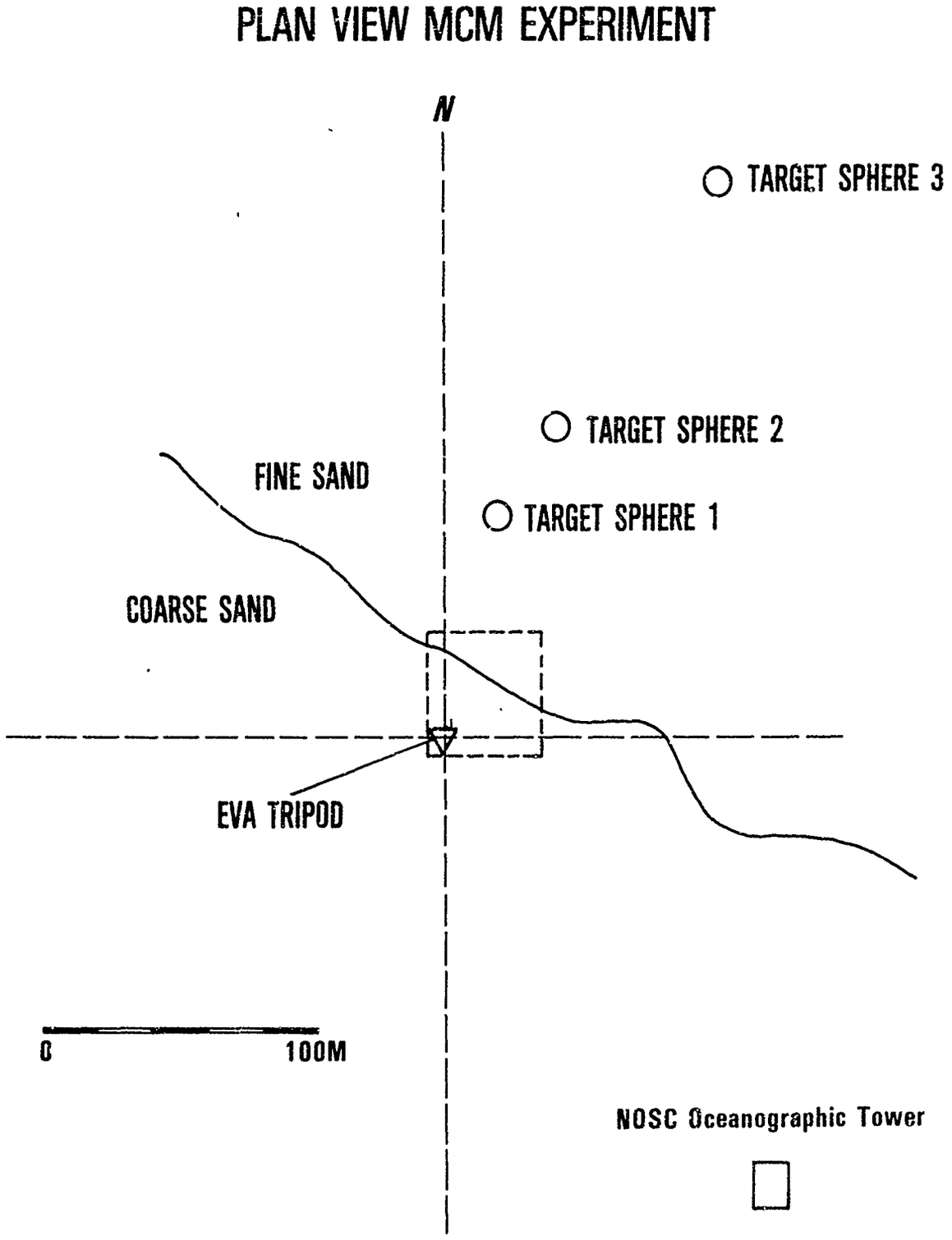

Figure 2. Plan view of experimental site showing location of the EVA tripod, NOSC Oceanographic Tower, three target spheres and division between fine and coarse sand substrates.

TABLE 1. SUMMARY OF DIVING (SCUBA) ACTIVITIES FOR THE NOSC TOWER EXPERIMENT

DIVE #	DATE	TIME (PST)	LOCATION	DIVE PURPOSE AND SAMPLES COLLECTED
1	29-4-82	1135-1146	tripod	photograph tripod
2	29-4-82	1219-1228	target sphere 2	2 sediment core samples (#3, 4)
3	29-4-82	1316-1323	target sphere 3	2 sediment core samples (#1, 5)
4	29-4-82	1350-1359	target sphere 1	2 sediment core samples (#6, 2)
5	30-4-82	1017-1042	target sphere 1	2 box cores for fauna
6	1-5-82	0932-1008	target sphere 3	stereo camera; sediment profiler
7	3-5-82	0955-1019	interface	stereo camera; sediment profiler; epifauna survey
8	3-5-82	1353-1423	near tripod	stereo camera; large scale survey mapping
9	3-5-82	1503-1513	interface	4 sediment core samples (#7-10)
10	4-5-82	0823-0848	near tripod	sediment profiler
11	4-5-82	1306-1337	between interface and target sphere 1	sediment profiler
12	5-5-82	0845-0909	target sphere 2	stereo camera, 3 sediment cores (#11-13)
13	5-5-82	1220-1235	near tripod	4 sediment cores (#14-17)
14	5-6-82	0826-0848	between tripod and target sphere 1	epifauna survey

cores were collected at the interface between the two substrate types (7-10); three cores were collected between the target sphere sites (11-13); and four cores were collected near the tripod (14-17) (Fig. 3). The core samples were returned to the NOSC Tower where compressional wave velocity and attenuation measurements were made. The cores were then sectioned for later physical properties analysis.

C. LABORATORY ANALYSIS

Sediment temperature was equilibrated to room temperature prior to acoustic measurements. Temperature and salinity of the overlying water were measured with a YSI Model 43TD temperature probe and a AO Goldberg temperature-compensated, salinity refractometer.

Values of sediment compressional wave velocity and attenuation were determined at 1 cm intervals in the core samples with an Underwater System, Inc. (Model USI-103) transducer-receiver head. A Tektronic PG 501 Pulse Generator and FG 504 Function Generator, Krohn-Hitz 3100R Band Pass Filter and a Hewlett Packard 1743A dual-time interval oscilloscope were substituted for the electronics unit and oscilloscope usually employed with the USI-103 Velocimeter (Fig. 4). These substitutes increased resolution of compressional wave velocity measurements and provided accurate measurement of received voltages required for attenuation measurements.

The transducer was driven with a 400 kHz, 20 volt p-p sine wave triggered for 25 us duration every 2 msec using the pulse generator and function generator. The received signal was filtered (1-1000 kHz high cut-off and low cut-off) prior to making time delay and received voltage measurements. Time delay measurements were made as the fourth sine wave first crossed the volts/division base line. Received voltage measurements were made utilizing the maximum peak height of the fourth sine wave.

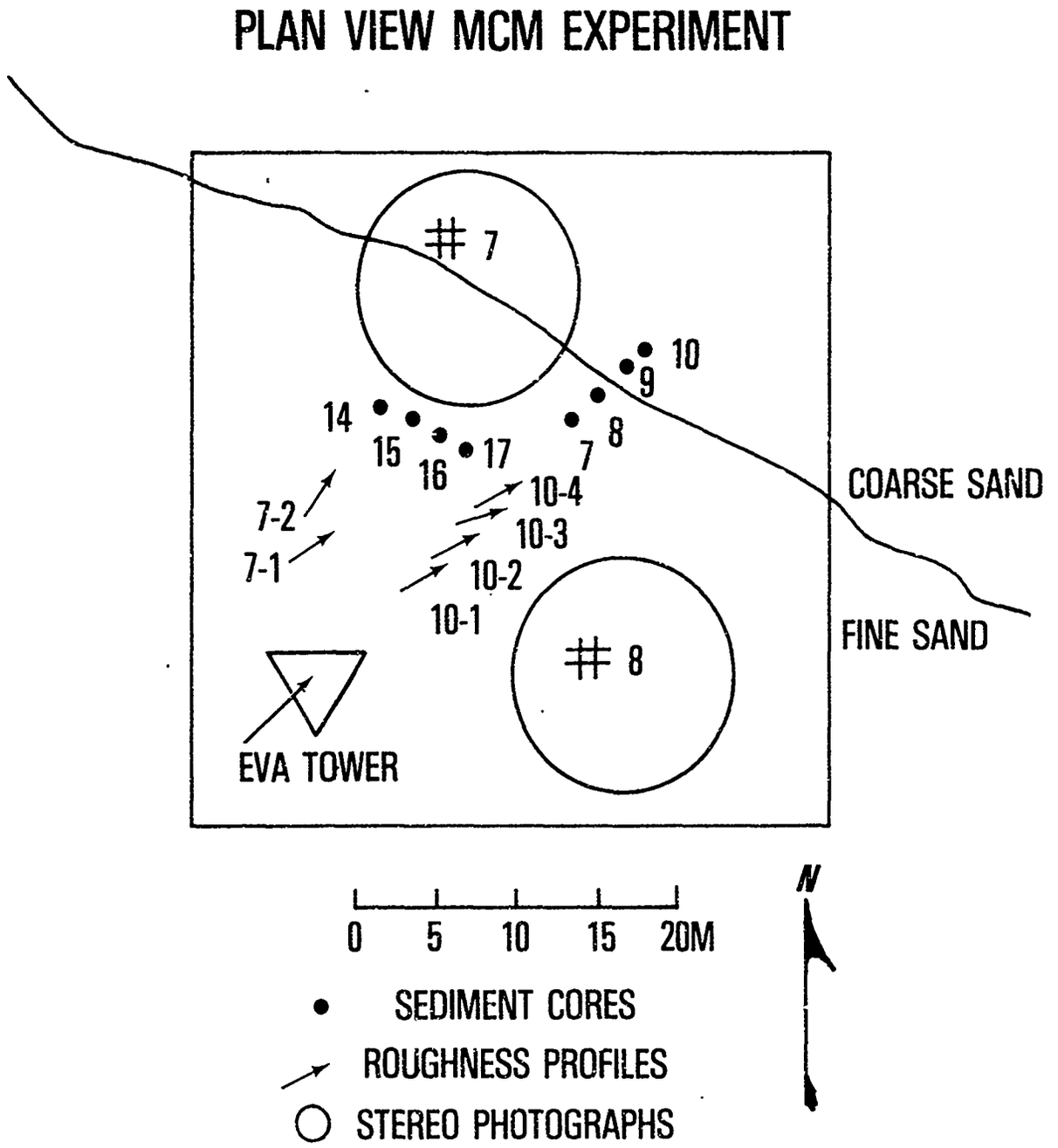

Figure 3. Plan view of part of experimental site near the EVA tower showing the sampling locations for sediment cores, roughness profiles and stereo photographs.

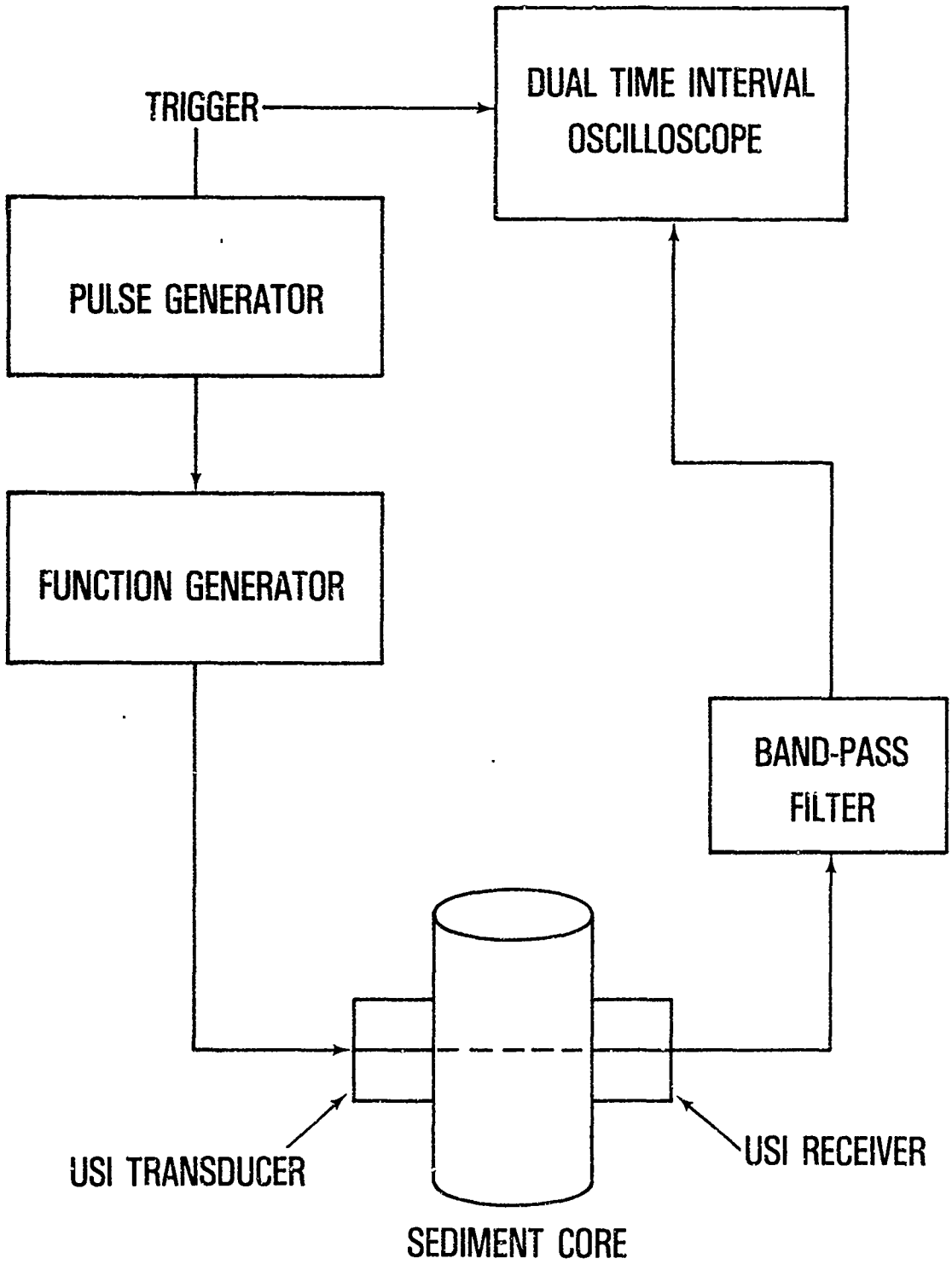

Figure 4. Block diagram of compressional wave velocity and attenuation measuring system.

Sediment compressional wave velocity was determined by comparison of similar time delay measurements made on distilled water and sediments using the following formula:

$$Cs = \frac{Cw}{1 - \frac{\Delta t C_w}{d}} \qquad (1)$$

where C_s is the measured sound velocity through sediment (m/sec); C_w is the measured sound velocity through distilled water (m/sec); Δt is the measured time arrival through sediment (sec); and d is the inside diameter of the core (m). All sound velocities were corrected to a common temperature, salinity, and pressure (23°C, 35 ppt, 1 atm) after Hamilton (1971).

Attenuation measurements were calculated as 20 log of the ratio of the received voltage through distilled water versus received voltage through sediment. Attenuation measurements were extrapolated to a 1 m path length and reported as dB/m (Hamilton, 1972). Attenuation was also expressed as a sediment specific constant (k):

$$a = kf^n \qquad (2)$$

where a is the attenuation of compression waves in sediment (dB/m), f is the transmitted signal frequency (kHz) and n is the exponent of frequency. If n is assumed to be one (Hamilton, 1972), then the sediment specific constant (k) can be used to compare sediment attenuation to other sediment physical properties such as porosity and mean grain size without regard to the frequency at which the measurements were made.

After acoustic measurements were made, sediment from 11 of the 17 cores was extruded and sectioned at 2 cm intervals for grain size analysis. Sediment grain size distribution was determined with an ATM Sonic Sifter for gravel and sand size particles and by pipette method to determine percent silt and percent clay. Mean phi, standard deviation, kurtosis, and

normalized kurtosis were calculated according to the graphic formula of Folk and Ward (1957).

III. RESULTS

A. SEDIMENT PHYSICAL PROPERTIES

Two sediment types were evident from visual (scuba) observations and from laboratory analysis of sediment grain size. The sediments closest to the tripod were coarser grained, dominated by to 1 Ø and 2 Ø modes, than the sediments surrounding the target spheres, which were dominated by the 4 Ø mode (Appendix A). Sediments surrounding the tripod (cores 14, 15, 16) were moderately to moderately well-sorted, fine-skewed, platykurtic to mesokurtic coarse grained sands. The sediments which surrounded the target spheres (cores 1, 2, 3, 11) were poorly sorted, very leptokurtic, fine to very fine sands, with surface sediments being fine-skewed while sediments at depth were near-symmetrical to coarse-skewed. The tendency towards coarser skewness with increased depth in cores 1, 2, 3, 11, reflected an increased percentage of the 1 Ø and 2 Ø sediment modes, that indicated some mixing of the two sediment types.

To determine the processes responsible for controlling the distribution of the two sediment types, four cores were collected at the interface between the two types (Fig. 3). Cores 8 and 9 were collected 1 m from either side of the sediment interface while cores 7 and 10 were taken 3 m from either side of the interface.

Sediments throughout the 18 cm length of core 7 were moderately sorted, very finely-skewed, platykurtic to mesokurtic coarse grained sands similar to sediments collected near the tripod. Except for the 4-8 cm depths, sediments throughout the 18 cm length of core 8 were also similar to sediments collected near

the tripod. Sediments from the 6-8 cm section contained a high percentage of the 4 Ø mode in addition to the 1 and 2 Ø modes. The result was a very poorly sorted, near-symmetrical, mesokurtic fine sand. The 4-6 cm section also contained both phi modes but was dominated by coarse grained sand.

Sediments found in the upper 4 cm of core 9 were poorly sorted, fine-skewed, leptokurtic, very fine sands dominated by the 4 Ø mode. These sediments were very similar to sediments collected near the target spheres. Sediments from the 6-8 cm section were very poorly sorted near-symmetrical, mesokurtic sand with an equal percentage of the 4 Ø and the 1-2 Ø modes. The bimodal distribution of grain size indicated an approximately even mixture of the two sediment types. Sediments from the 6-8 cm section were poorly sorted, strongly coarse-skewed very leptokurtic medium sand which indicated a small contribution of the fine-grained sediments. The remaining sediments (8 to 16 cm depth) were moderately sorted, fine-skewed leptokurtic coarse sands dominated by the 1 Ø and 2 Ø modes. These sediments were identical to the coarse-grained sediments found near the tripod. Sediments from the upper 16 cm of core 10 were poorly sorted, strongly fine-skewed, mesokurtic to leptokurtic coarse silt dominated by the 4 Ø mode. These sediments were almost identical with the fine-grained sediment found near the target spheres. The 16-18 cm sediment section was a poorly sorted, near symmetrical, leptokurtic very fine sand resulting from a mixture of both substrate types.

Sediments found near the tripod had coarser mean grain size values (~1.0 Ø) than sediments surrounding the target spheres (~3.5 Ø) (Fig. 5). Patterns of mixing of the two sediments at their interface were also demonstrated by mean grain size distributions (Fig. 6). The sediments from core 7 were coarse sands. Sediments from core 8 were predominately coarse sands with an inclusion of fine sand material at 6-8 cm. The upper 4 cm of core 9 was comprised of fine sands with a mixture of the two

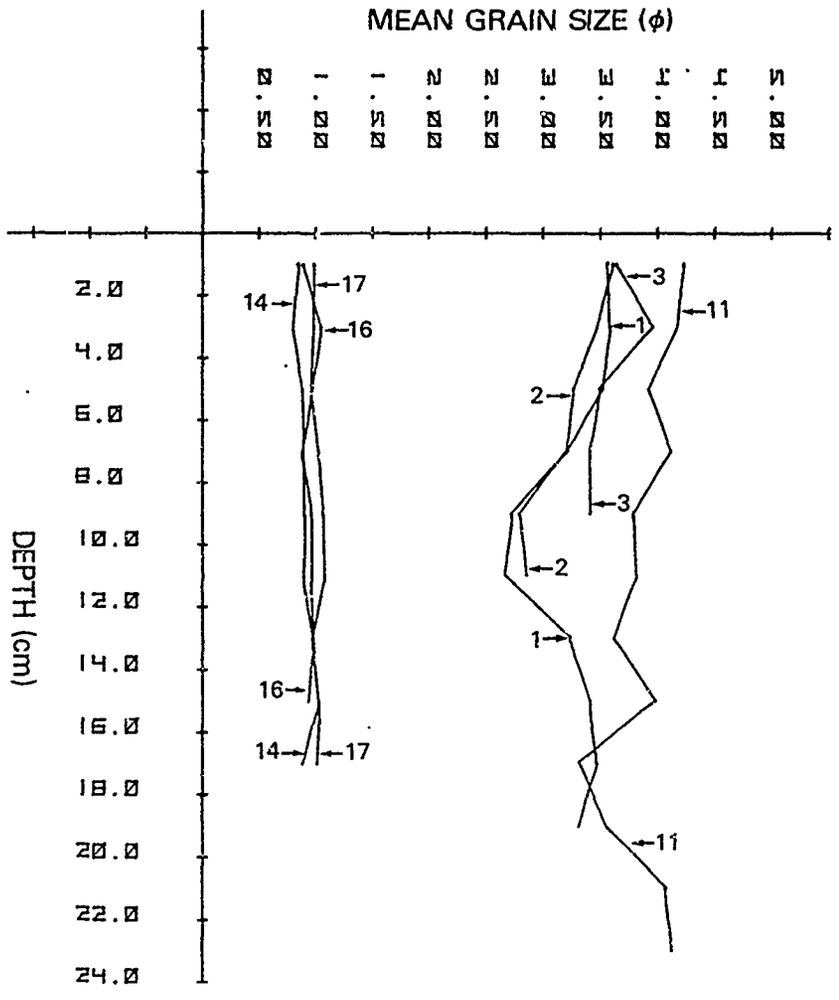

Figure 5. Vertical distribution of sediment mean grain size for cores 1, 2, 3, 11, 14, 16 and 17.

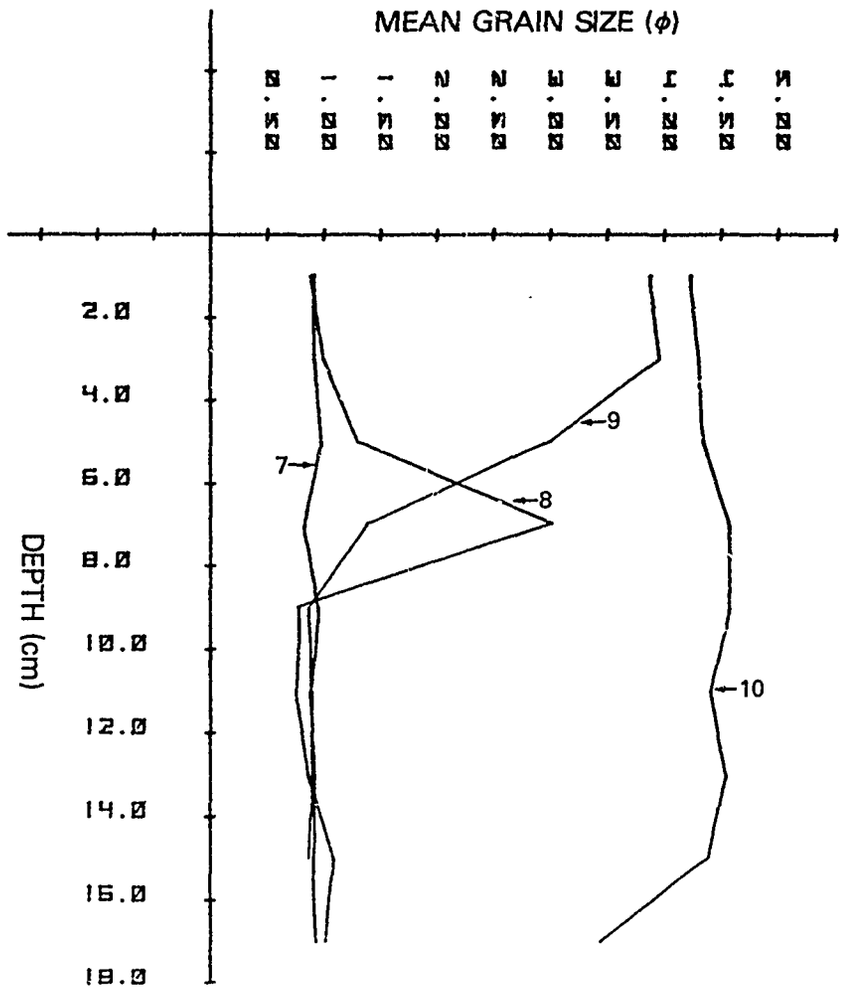

Figure 6. Vertical distribution of sediment mean grain size for cores 7, 8, 9 and 10.

sediment types from 4 to 8 cm and a domination of coarse sands to 18 cm. Core 10 was predominately fine sands with an indication of slightly coarser material in the 14-16 cm section.

B. SEDIMENT ACOUSTIC PROPERTIES

Sediment compressional wave velocity (m/sec), velocity ratio, and attenuation, expressed as (dB/m @ 400 kHz), and k were calculated at 1 cm intervals for 17 cores collected from the experimental site (Appendix B). Compressional wave velocity was calculated for a common depth (0 m), temperature (23°C) and salinity (35 ppt) after the suggestion of Hamilton (1971). In situ compressional wave velocity for 18 m depth, 34 ppt salinity and the range of temperatures encountered in this study can be calculated by multiplication of the velocity ratio by conversion factors in Table 2.

Sediment compressional wave velocity ratio was much higher (mean, 1.15) in the coarser grained sediments near the tripod (cores 14, 15, 16, 17) than in the finer grained sediments (mean 1.10) surrounding the target spheres (cores 1, 2, 3, 4, 5, 6, 11, 12, 13). Except for three data points there was no overlap in V_p ratio values (Fig. 7). There was an approximate 2% increase in velocity ratio from core top to bottom for both sediment types. The V_p ratio corresponded to compressional wave velocity of 1757 m/sec in the coarse sand sediment and 1681 m/sec in the fine sand sediments (for 23°, 35 ppt, 0 m). The 2% increase in velocity ratio corresponded to a 30 m/sec increase in velocity with 20 cm increase in depth.

Sediment attenuation at 400 kHz was much higher in fine sand sediments surrounding the target spheres (194 dB/m) than in coarse sand sediments surrounding the tripod (115 dB/m). Little overlap was evident between depth distributions of attenuation coefficient (k) for finer grained sediments (cores 1, 2, 3, 4, 5, 6, 11, 12, 13) and those for coarser grained sediments (14, 15, 16, 17) (Fig.

TABLE 2. Compressional wave velocity for seawater at 34 ppt salinity and 18 m depth for the range of in situ bottom temperatures encountered in the NOSC Tower Experiment and for 23°C (MacKenzie, 1981).

T°C	V_p (m/sec)
10	1488.7
11	1492.2
12	1495.7
13	1499.2
14	1502.4
15	1505.7
16	1508.9
17	1511.8
18	1514.8
19	1517.6
23	1528.3

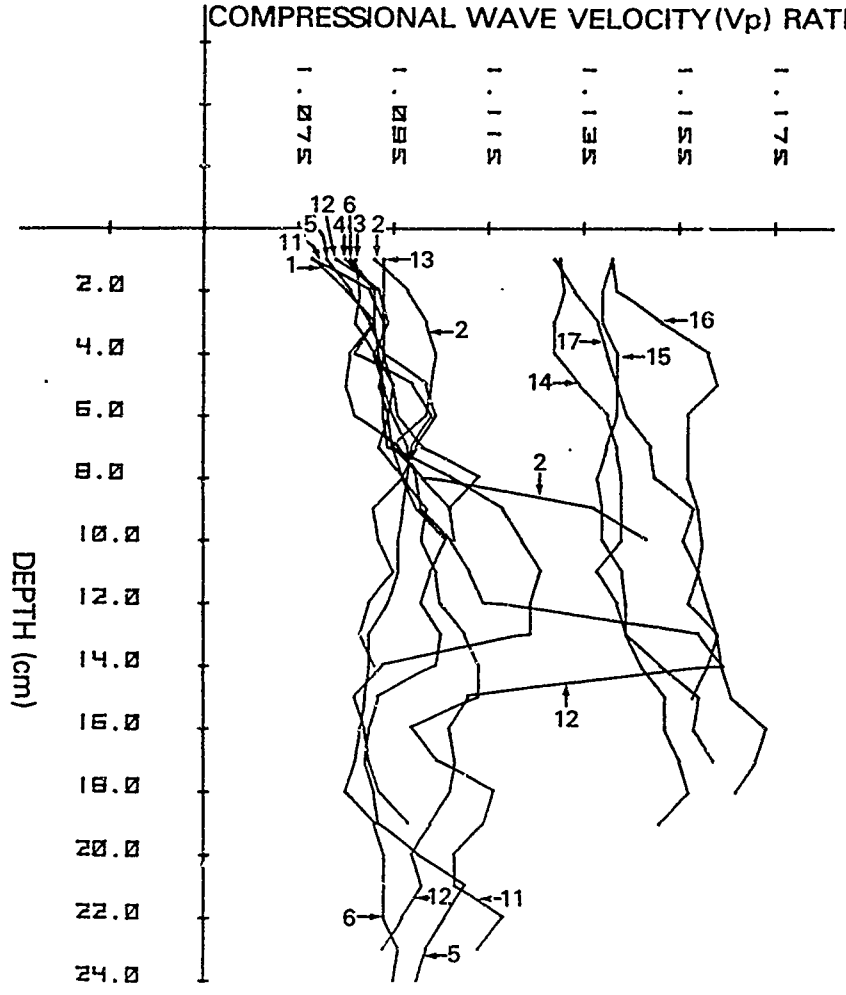

Figure 7. Vertical distribution of sediment velocity ratios (V_p) for cores 1-6 and 11-17.

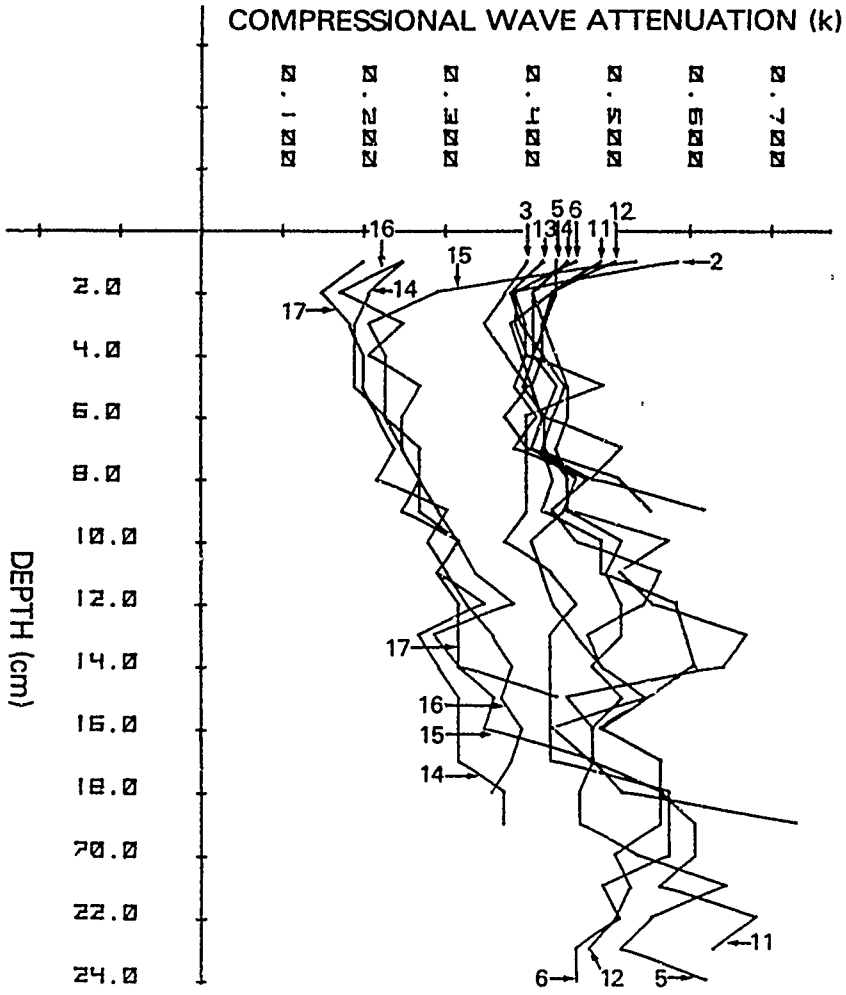

Figure 8. Vertical distribution of compressional wave attenuation (k) for cores 1-6 and 11-17.

8). There was an approximate 0.15 unit increase in k values with depth for all core samples which corresponded to a 60 dB/m (at 400 kHz) increase in attenuation with 20 cm increase in depth.

Compressional wave velocity ratios measured on cores taken at the interface of the two substrates varied inversely with mean grain size values (Fig. 9). Compressional wave velocity ratio at station 10 (1.07) was approximately the same as for fine grained sediments found near the target spheres. The V_p ratios measured for upper 5 cm of sediment in core 9 were similar to V_p ratios from other fine sands, and at 6-8 cm depth they had increased to values similar to those for coarse sands. V_p ratio values for sediments in core 8 were similar to those for coarse sands, except for a lower V_p ratio for sediments from 7 to 8 cm depth which corresponded to the mixture of fine and coarse sands found there. Sediments in core 7 also had high velocity ratio values except for sediments from the 8-10 cm section.

Depth distribution of attenuation measurements calculated for sediments at the interface of the two substrate types did not correlate with depth distribution of V_p ratio or mean grain size (Fig. 10). In general, attenuation was higher than would be expected from knowledge of distribution of grain size.

IV. DISCUSSION

A. VARIABILITY OF SEDIMENT GEOACOUSTIC PROPERTIES

It has been shown that sediment geoacoustic properties such as compressional wave velocity, sediment mean grain size and sediment porosity can be quite variable in shallow coastal marine silty-clay sediments (Richardson et al. 1983). The within-core variability (Figs. 5, 7 and 8) of sediment geoacoustic properties (compressional wave velocity and attenuation and mean grain size) appears to be much lower in the sandy sediments encountered in

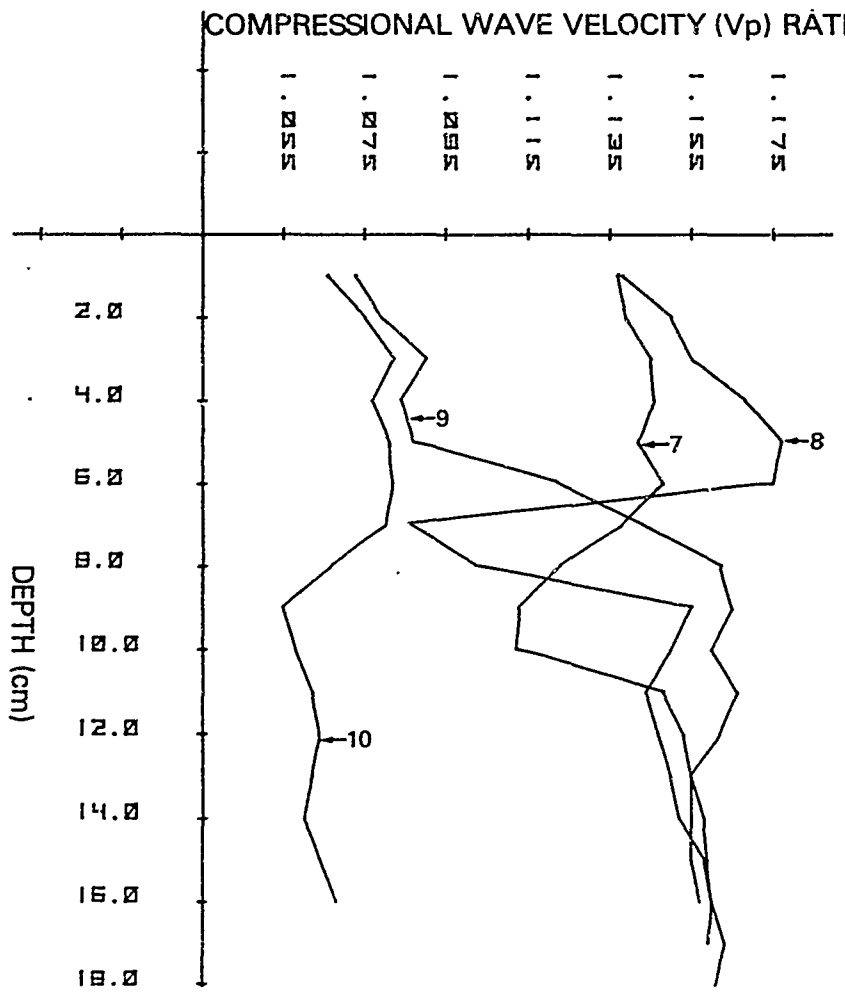

Figure 9. Vertical distribution of sediment velocity ratio (V_p) for cores 7, 8, 9 and 10.

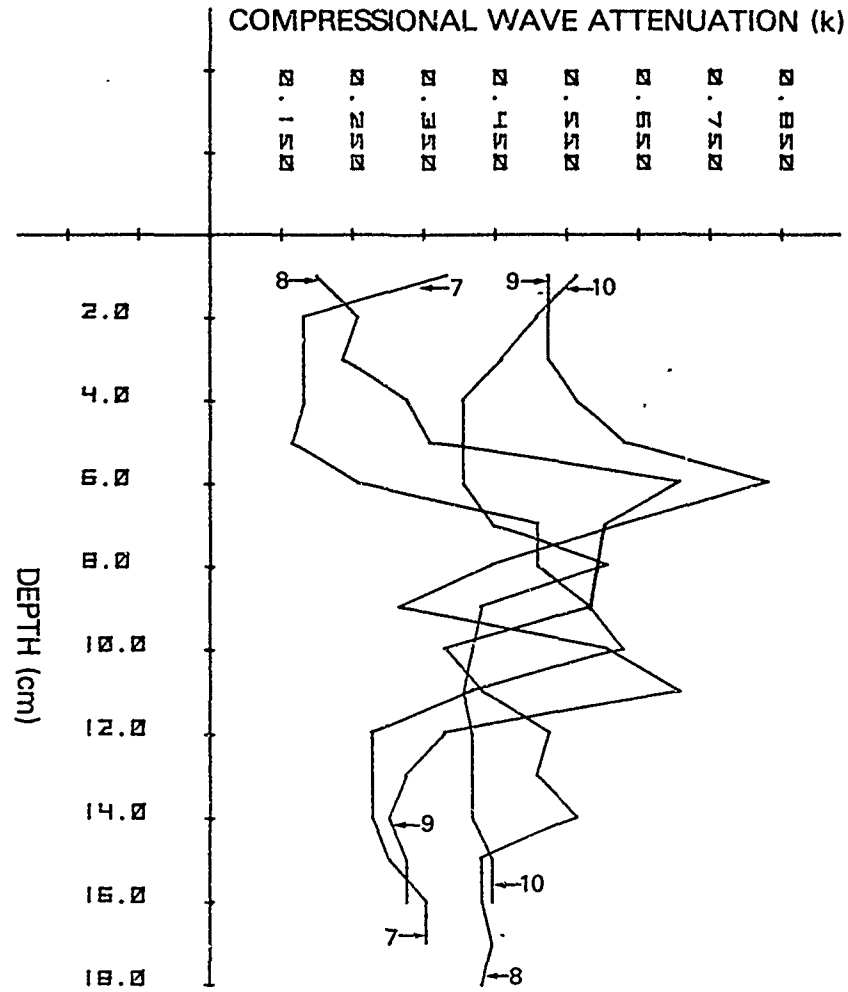

Figure 10. Vertical distribution of compression wave attenuation (k) for cores 7, 8, 9 and 10.

this study compared with that in the silty-clay sediments studied by Richardson et al. (1983). Sediment cores collected at the interface between the two substrate types (cores 7-10) had the most variation in geoacoustic properties because they contained mixtures of both sediment types. Between-core variability of sediment geoacoustic properties for samples collected in the same substrate type was also much lower in this sandy substrate than within-station variability of these properties in silty-clay sediments. We can, therefore, predict sediment geoacoustic properties of the insonified portion of the substrate with much greater accuracy around the NOSC Oceanographic Tower than in silty-clay sediments from Long Island Sound.

The variability of geoacoustic properties was slightly less for the coarser sediments found near the tripod than for the finer sediments surrounding the target spheres (Fig. 11; Table 3). The variance of the velocity ratio and attenuation can be further reduced by assuming gradients of increased velocity and attenuation with depth (Figs. 12, 13 and Table 3).

B. PREDICTION OF IN SITU SEDIMENT IMPEDANCE AND ATTENUATION

Mean values, variability, and gradients of measured geoacoustic properties were used to calculate in situ sediment impedance and attenuation. These values are required as inputs to predict backscatter coefficients for the frequencies used in this experiment.

Density, $\rho(g/cm^3)$, was predicted using the density versus mean grain size, M_z (ϕ) predictor equation given for continental shelf sediments (Hamilton and Bachman, 1982).

$$\rho = 2.374 - 0.175M_z + 0.008M_z^2 \qquad (3)$$

Impedance ($g/cm^{-2}sec \cdot 10^5$) was then calculated as the product of density and compressional wave velocity. Sediment impedance (I)

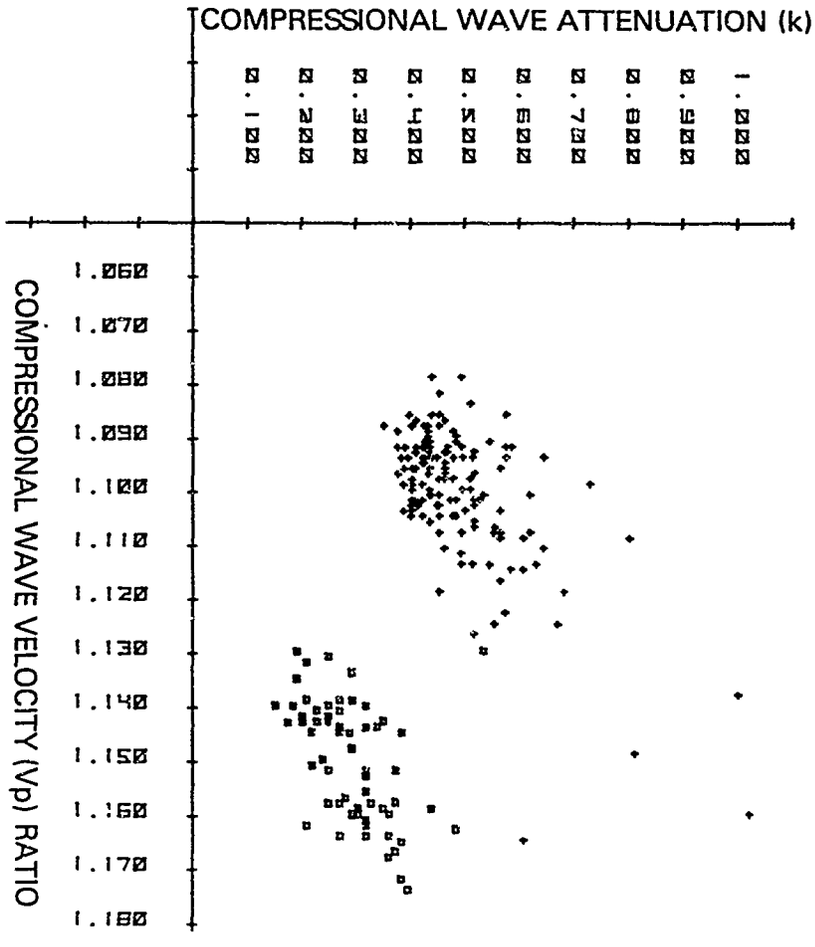

Figure 11A. Scatter plots of sediment geoacoustic properties for fine (+) and coarse (o) sand sediments; attenuation vs velocity ratio.

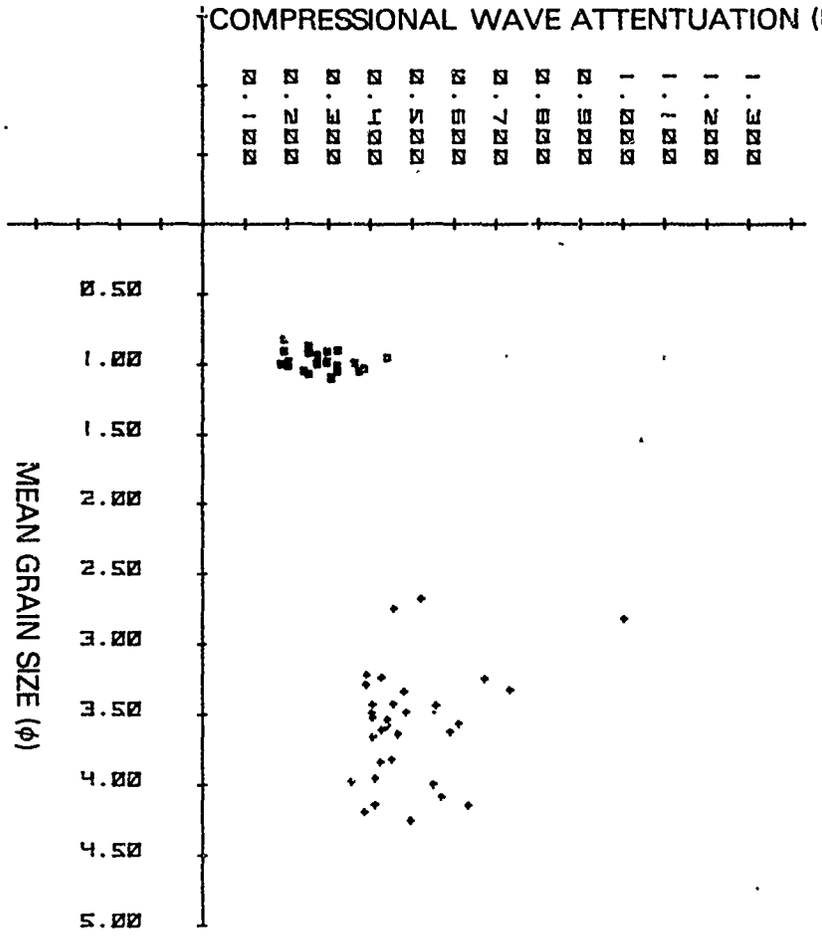

Figure 11B. Scatter plots of sediment geoacoustic properties for fine (+) and coarse (o) sand sediments; attenuation vs mean grain size.

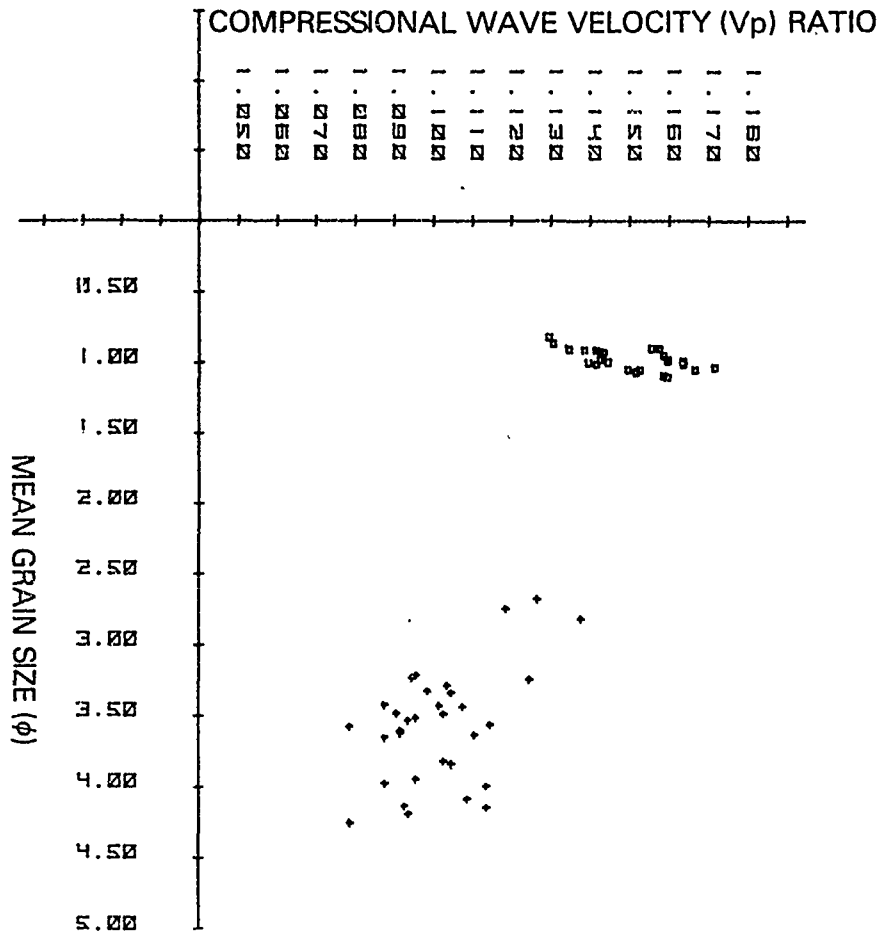

Figure 11C. Scatter plots of sediment geoacoustic properties for fine (+) and coarse (o) sand sediments; velocity ratio vs mean grain size.

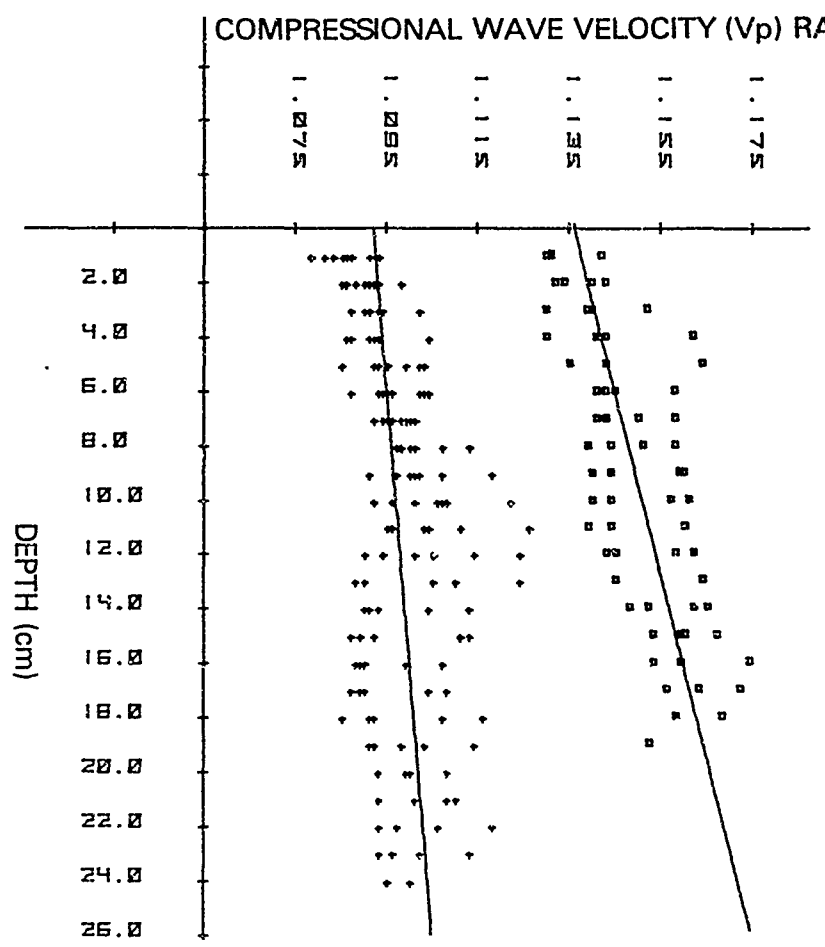

Figure 12. Regression of velocity ratio with depth for fine (+) and coarse (o) sand sediments.

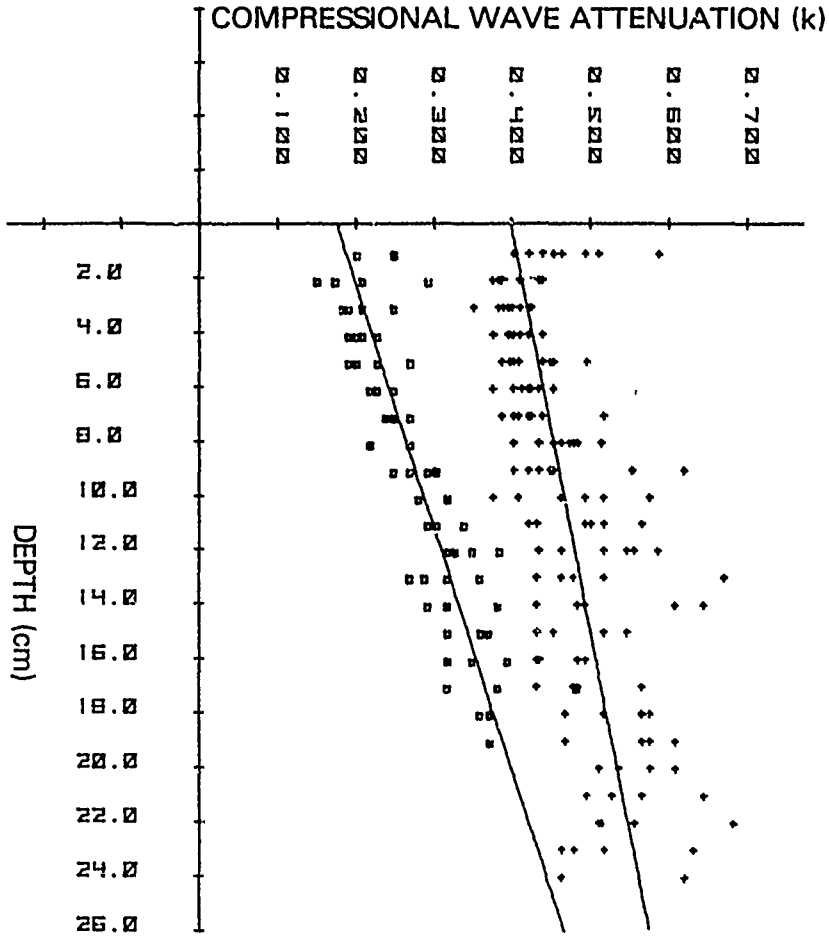

Figure 13. Regression of attenuation with depth for fine (+) and coarse (o) sand sediments.

TABLE 3. Variability of sediment geoacoustic properties for the fine and course sand sediments encountered near the NOSC Oceanographic Tower (F = statistics for mean square of V_p ratio or k explained by gradient).

	V_p ratio		k		Mean Grain Size	
	coarse	fine	coarse	fine	coarse	fine
Mean	1.1489	1.0987	0.2868	0.4722	0.957	3.533
Variance	0.0001	0.0002	0.0054	0.0060	0.005	0.172
Standard Deviation	0.0111	0.0127	0.0738	0.0775	0.071	0.415
Skewness	0.0922	2.1969	0.6954	1.2390	-0.193	-0.244
Kurtosis	1.9886	10.4485	3.7066	4.7797	2.171	2.415
Gradient/cm	0.0015	0.0005	0.0112	0.0067	--	--
Residual mean square of regression	0.00007	0.00008	0.00117	0.00297	--	--
F-statistic	54.3***	21.4***	179.4***	98.6***	--	--

*** F significant at 0.001 level

can easily be calculated for in situ temperatures other than 15°C by multiplication of impedance ($I_{15°}$) by the compressional wave velocity (V_p) at the desired temperature divided by 1505.7 m/sec.

$$I = \frac{I_{15°} \cdot V_p}{1505.7} \qquad (4)$$

Both sediment density and impedance were lower in the coarse sand sediment found near the tripod (Table 4). The variability of sediment density and impedance was highest for the fine sand sediments surrounding the target spheres. The gradient of increased density and impedance with depth was computationally controlled by the gradients of compressional wave velocity because no gradient in sediment mean grain size was evident (Figs. 14 and 15).

The attenuation of compressional waves at frequencies used in this experiment can be calculated if the exponent of frequency (n) in equation (2) is assumed to be 1 (Hamilton, 1972). The measured and calculated attenuation values were in all cases highest in the fine sand sediments which surround the target spheres. The attenuation values and gradients (Table 5) can be used to calculate the effective depth of penetration of compressional waves at various frequencies for this experiment.

C. CORRELATIONS BETWEEN SEDIMENT GEOACOUSTIC PROPERTIES

Correlations between sediment geoacoustic properties were greater for all data combined than for data of individual substrate types separately (Table 6). The low variability of sediment geoacoustic properties within substrate types tended to produce two clusters of points (Figs. 16 and 17) while correlations between all data points produced the true relationships between parameters over a wider variety of sediment types (Fig. 18). The regressions between sediment compressional

TABLE 4. Variability and gradients with depth of density (g/cm^3) and impedance ($g/cm^2 sec \cdot 10^5$) of sediments encountered near the NOSC Oceanographic Tower (F-statistic for mean square of sediment density and impedance explained by gradient).

	Sediment Density		Sediment Impedance	
	coarse sand	fine sand	coarse sand	fine sand
Mean	2.2138	1.8569	3.0745	3.8351
Variance	0.0001	0.0025	0.0110	0.0001
Standard Deviation	0.0114	0.0496	0.1048	0.0308
Skewness	0.1871	0.3648	0.8565	0.2472
Kurtosis	2.1969	2.5269	3.5800	1.4606
Gradient/cm	-0.0007	0.0004	0.0038	0.0034
Residual mean square of regression	.0001	0.0025	0.0006	0.0109
F-statistic	2.29	0.09	16.25**	1.36

** F value significant at 0.01 level

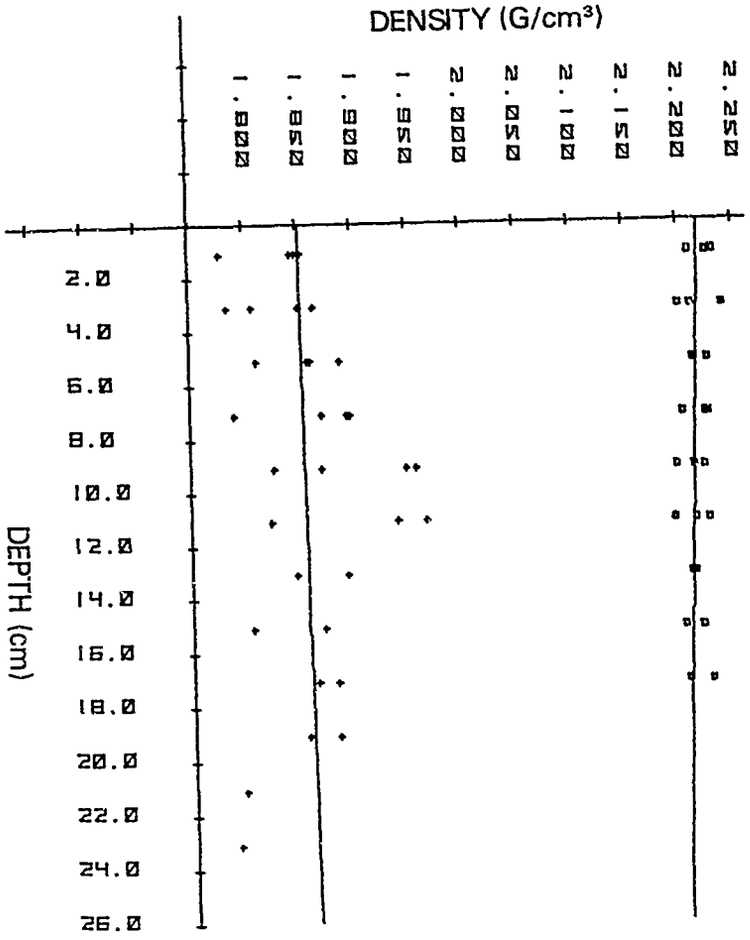

Figure 14. Regression of sediment density with depth for fine (+) and coarse (o) sand sediments.

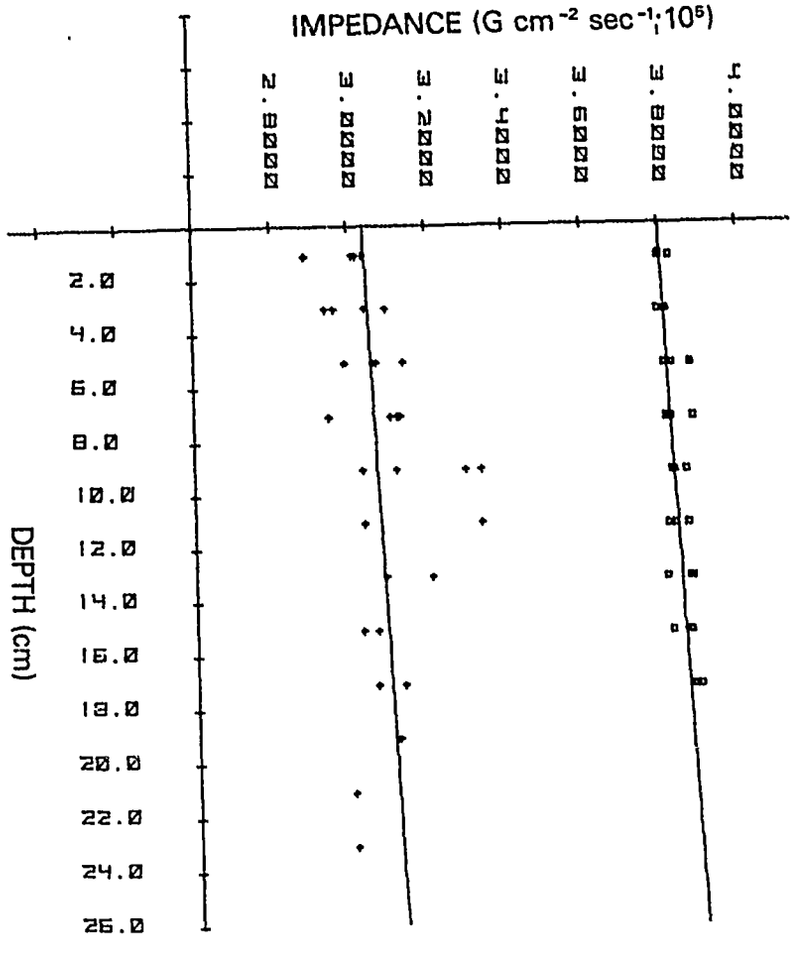

Figure 15. Regression of sediment impedance with depth for fine (+) and coarse (o) sand sediments.

TABLE 5. Calculated and measured mean values of sediment compressional wave attenuation (dB/m) for frequencies used in the NOSC Tower Experiment. Confidence limits around mean values for $t_{.05}$.

Frequency (kHz)	Fine Sand	Coarse Sand	Approximate Increase (dB/m) for 20 cm increase depth
30	14.6 ± 0.5	8.6 ± 0.5	5
45	21.9 ± 0.8	12.9 ± 0.8	7
60	29.2 ± 1.1	17.2 ± 1.0	9
80	38.9 ± 1.5	23.0 ± 1.4	12
95	46.2 ± 1.7	27.3 ± 1.7	14
400	194.0 ± 7.3	114.8 ± 7.0	60

TABLE 6. Correlations between measured sediment geoacoustic properties compressional wave velocity (V_p) ratio and attenuation (k) and mean grain size (Ø) for all cores combined and coarse sand and fine sand cores separately.

Comparisons	All Cores	Coarse Sand	Fine Sand
V_p ratio - Ø	-0.912	0.589	-0.486
size F value (d.f.)	445.7 (90)	12.7 (24)	9.4 (30)
k - V_p Ratio	-0.826	0.482	0.602
F value (d.f.)	34.4 (290)	20.3 (67)	87.3 (154)
k - Ø	0.491	0.298	-0.288
F value (d.f.)	28.6 (90)	2.3 (24)	2.7 (30)

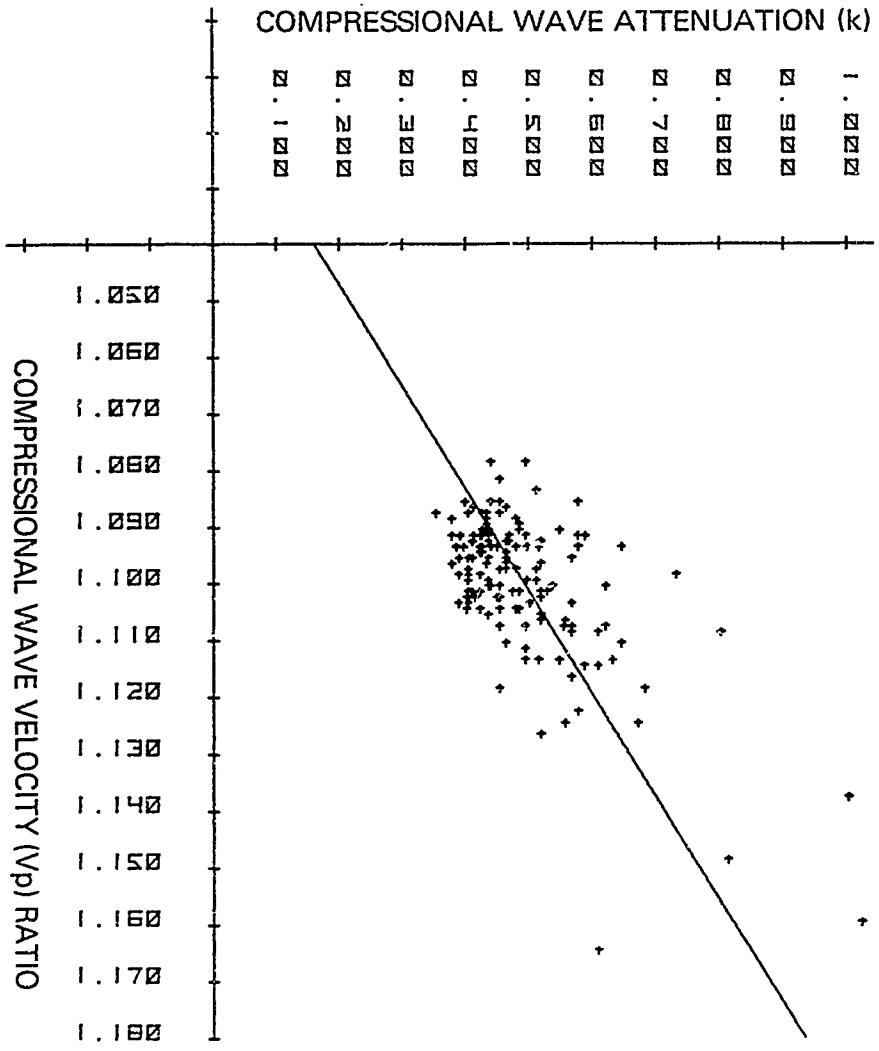

Figure 16A. Regression of sediment geoacoustic properties for fine sand sediments; attenuation with velocity ratio.

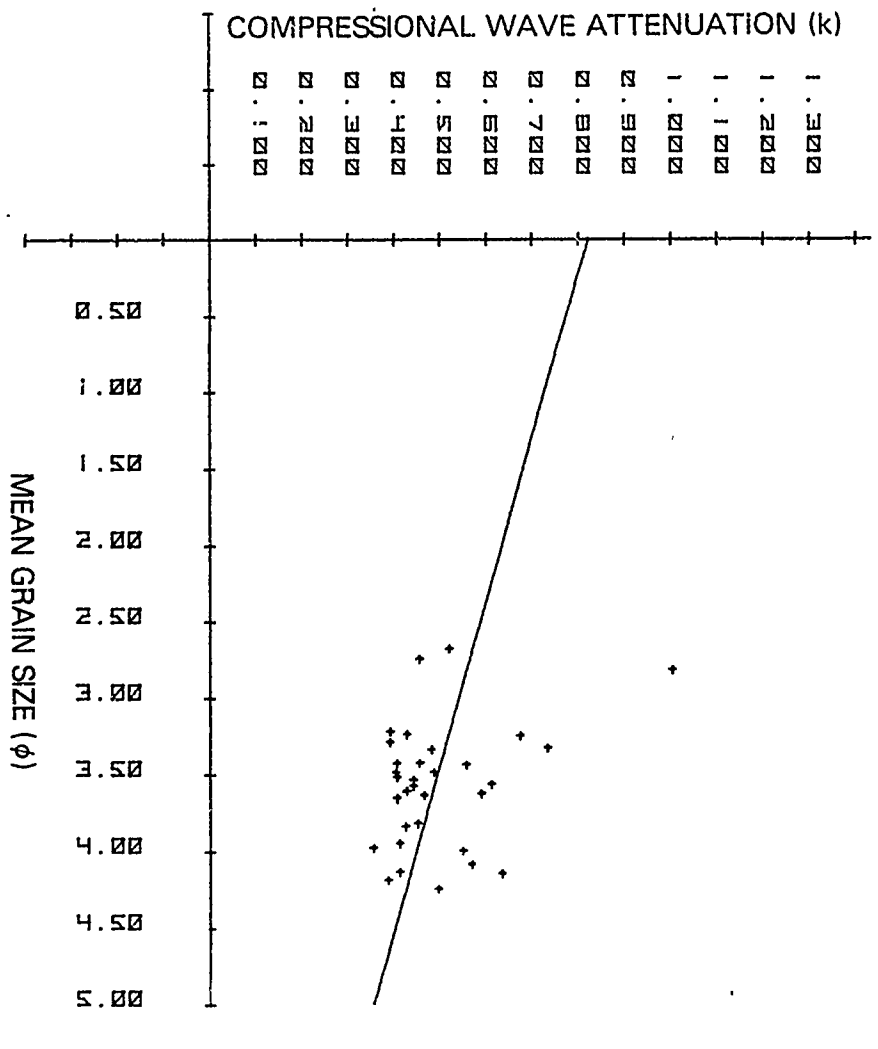

Figure 16B. Regression of sediment geoacoustic properties for fine sand sediments; attenuation with mean grain size.

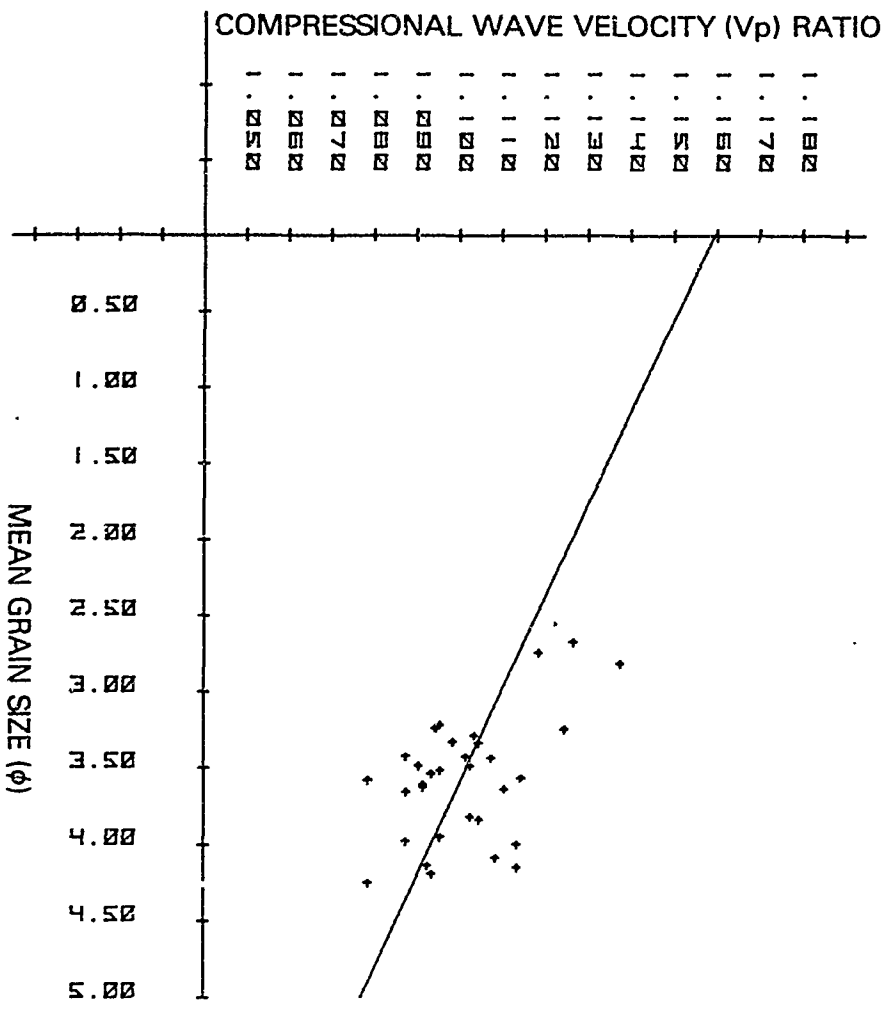

Figure 16C. Regression of sediment geoacoustic properties for fine sand sediments; velocity ratio with mean grain size.

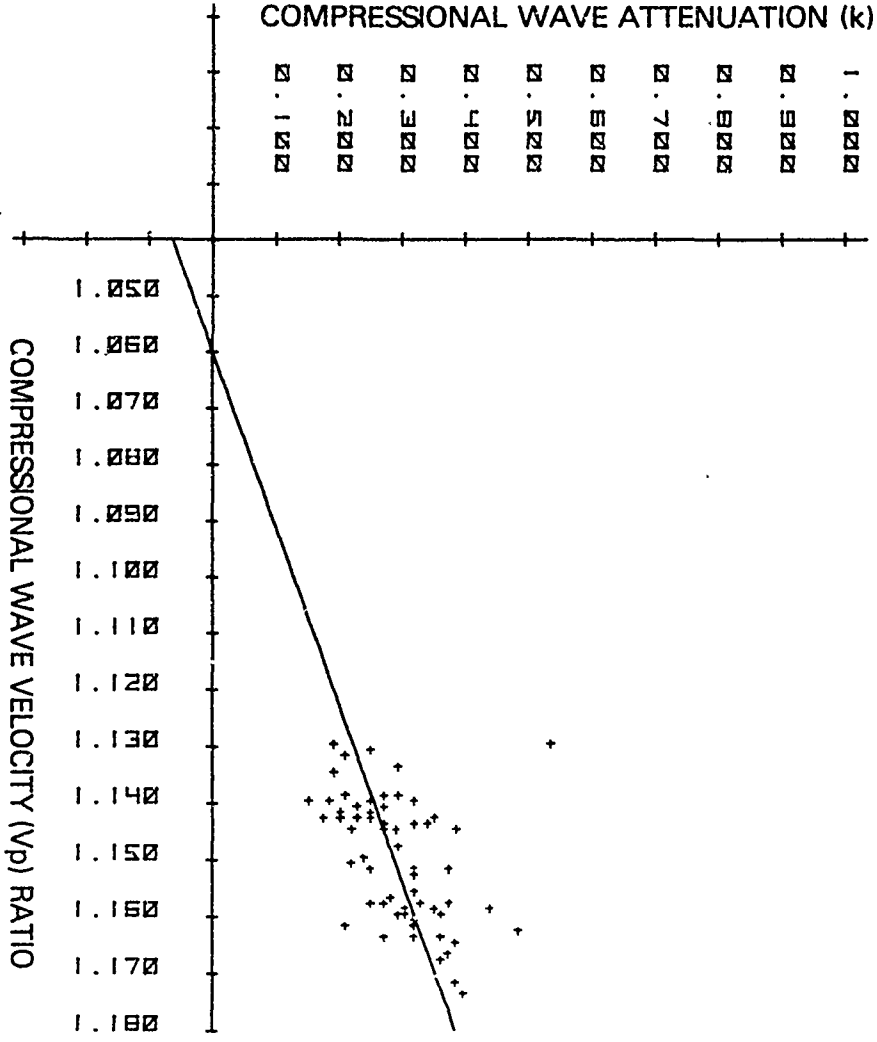

Figure 17A. Regression of sediment geoacoustic properties for coarse sand sediments; attenuation with velocity ratio.

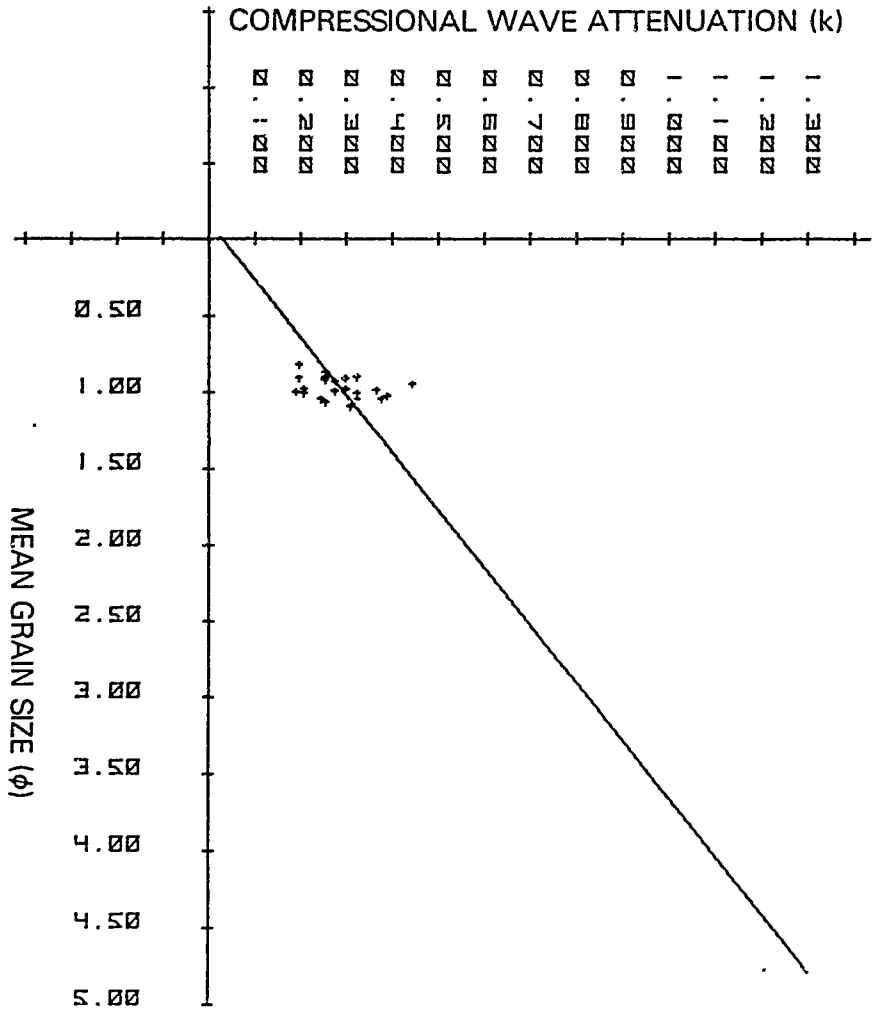

Figure 17B. Regression of sediment geoacoustic properties for coarse sand sediments; attenuation with mean grain size.

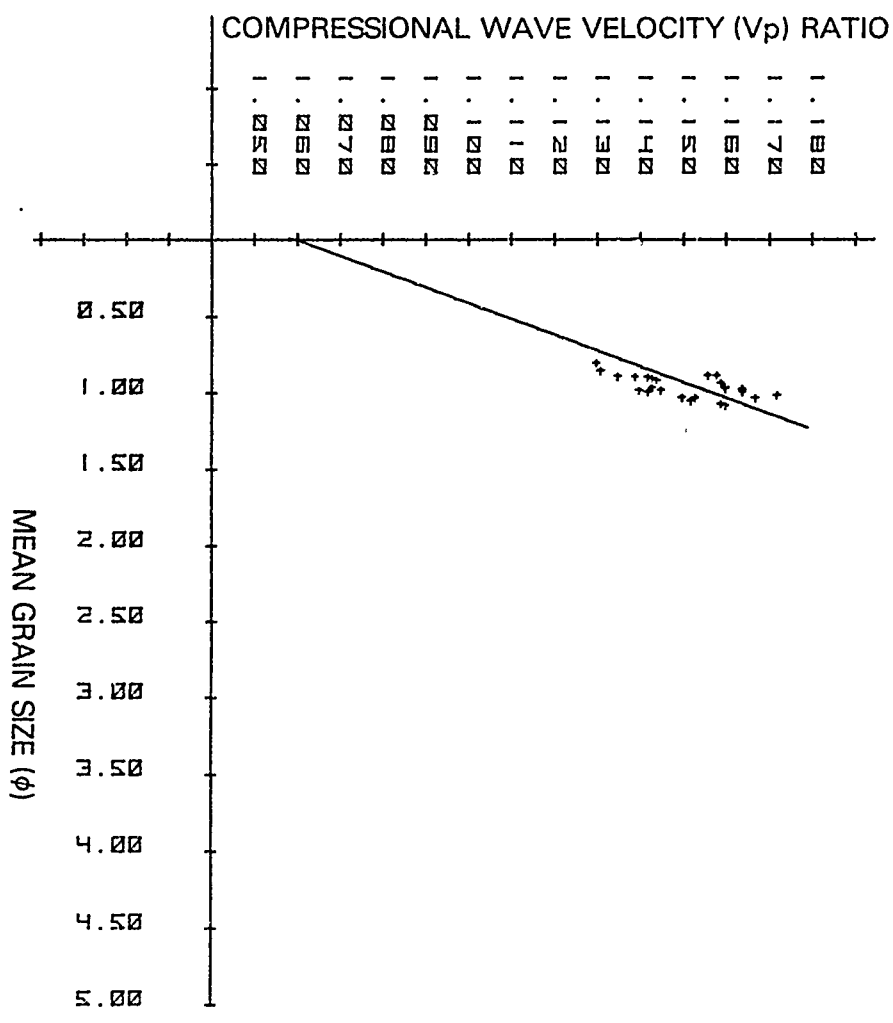

Figure 17C. Regression of sediment geoacoustic properties for coarse sand sediments; velocity ratio with mean grain size.

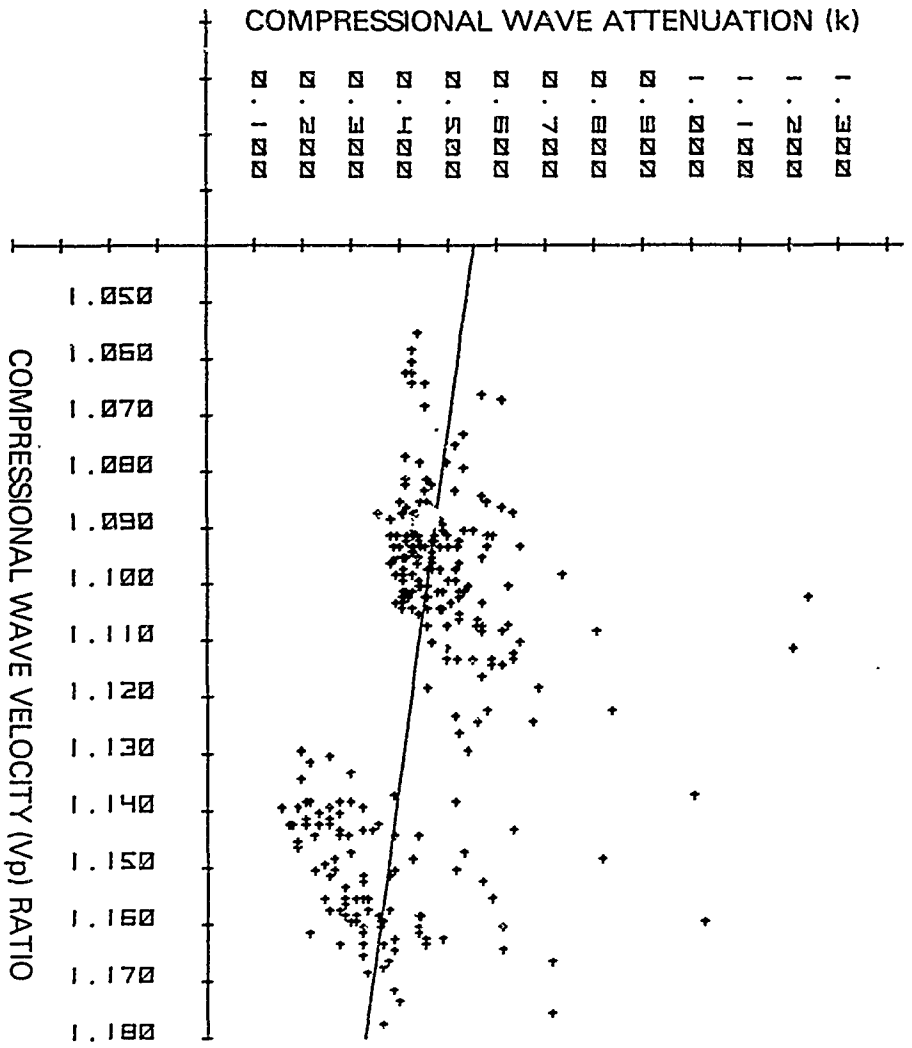

Figure 18A. Regression of sediment geoacoustic properties for all sediments combined; attenuation with velocity ratio.

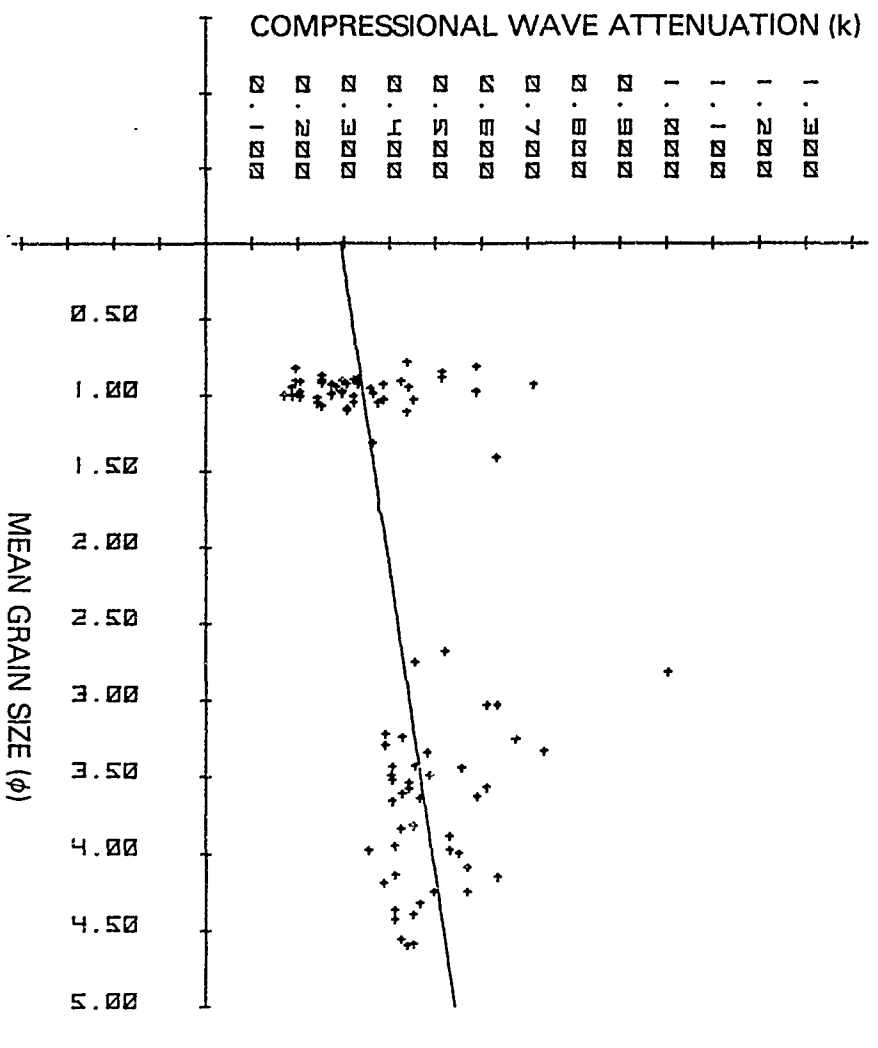

Figure 18B. Regression of sediment geoacoustic properties for all sediments combined; attenuation with mean grain size.

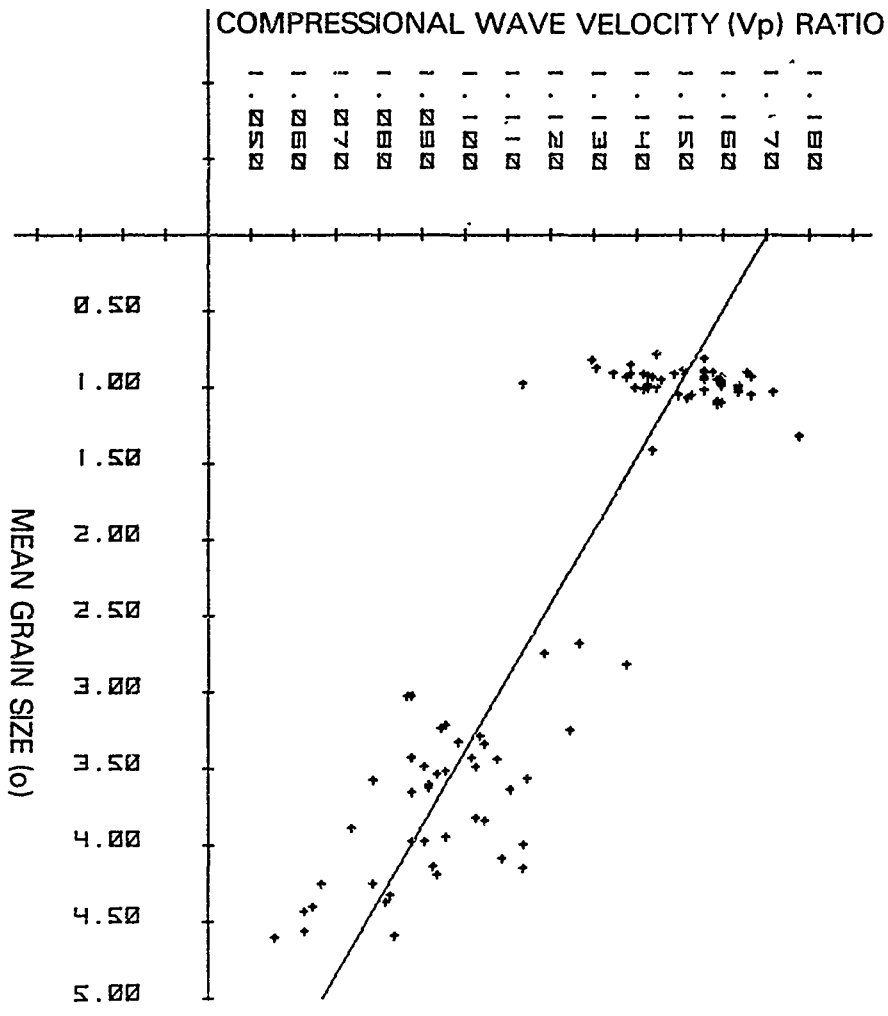

Figure 18C. Regression of sediment geoacoustic properties for all sediments combined; velocity ratio with mean grain size.

wave velocity and attenuation for separate sediment types reflect a simultaneous increase in both without commensurate increase in mean grain size. In fact, the correlation coefficient between compressional wave velocity and attenuation is negative for all cores combined and positive for the separate substrate types. This anomaly can be explained by assuming an increase in porosity with depth by compaction or packing processes without a concomitant change in mean grain size. This would produce an increase in compressional wave velocity and attenuation with depth while preserving the negative correlation between the two over a range of mean grain size. Unfortunately, porosity was not measured in this study.

D. COMPARISON WITH GEOACOUSTIC PREDICTOR EQUATIONS

Numerous empirical predictor equations between sediment acoustic and physical properties have been developed by the simultaneous measurement of both properties (Nafe and Drake, 1963; Horn et al., 1968; Buchan et al., 1972; Anderson, 1974 for example). The most recent and comprehensive are those of Hamilton and Bachman (1982) for prediction of compressional wave velocity and Hamilton (1980) for prediction of attenuation. Comparisons between Hamilton's predictor equations and our measured values are presented in Table 7.

Measured and predicted mean compressional wave velocities were nearly identical for fine sands encountered in this study but measured values were much lower than predicted values for coarse sands. Measured attenuation (k) values were also lower than predicted for both sediment types, but within Hamilton's envelope of predicted values (Hamilton, 1980).

Differences in measured and predicted values of compressional wave velocity and attenuation could result from several sources: first, differences in measurement technique; second, natural variability in values of these parameters; third, paucity of data

TABLE 7. Comparison of measured and predicted sediment acoustic properties for fine sands and coarse sands collected near the NOSC Oceanographic Tower. Predicted values based on equations given by Hamilton and Bachman (1982) and Hamilton (1980).

Parameter	Fine Sand		Coarse Sand	
	Measured	Predicted	Measured	Predicted
Mean Grain Size (Ø)	3.5	--	1.0	--
Compressional Wave Velocity (m/sec)	1681	1701	1758	1870
Velocity Ratio	1.099	1.112	1.149	1.222
Attenuation (k)	0.47	0.63	0.29	0.48

from shallow-water coarse sand sediments in construction of predictor equations; fourth, biological or hydrodynamic processes altering sediment acoustic properties; fifth, sediment disturbance during collection; or sixth, any combination of the above. Some insight into these differences can be obtained by comparison with data previously collected at the NOSC Tower and included in Hamilton's predictor equations.

Hamilton et al. (1970) reported diver (SCUBA) in situ measurements of compressional wave velocity and attenuation made at the NOSC Oceanographic Tower. Measurements were made over pathlengths of 0.6, 5.2, 9.8 and 14.3 m at a depth of approximately 30 cm. The sediment was 100% sand with a mean grain size of 0.495 mm (~1.0Ø). In situ bottom water velocity was 1501 m/sec and sediment velocity was 1798 m/sec. This yields a velocity ratio of 1.197 or 1832 m/sec at 23°C, 35 ppt and 0 m depth; much higher than the mean, 1758 m/sec, value for coarse sands in this study. Attenuation was 7 dB/m at 14 kHz for a calculated k value of 0.5 which was also much higher than the 0.28 reported for coarse sands in this study. The deepest penetration for cores collected in coarse sand for this study was 18 cm. Velocity ratio at that depth ranged from 1.15 to 1.17 or 1759 to 1790 m/sec compressional wave velocity. Attenuation (k) at that depth was 0.3 to 0.4. Using the regression equations in Figure 10, the projected compressional wave velocity at 30 cm would be 1802 m/sec (V_p ratio 1.179) and the attenuation (k) would be 0.51. These values are the same as measured by Hamilton et al. (1970).

Additional measurements are required to determine if the gradient in acoustic properties with no change in sediment grain size as measured in this study can account for the variability of geoacoustic predictor equations for shallow-water sandy substrates. Deep-water sediments (Richardson, in press) and shallow-water silty-clay sediments (Richardson et al., 1983) do not exhibit such acoustic gradients.

V. REFERENCES

Anderson, R. S. 1974. Statistical correlation of physical properties and sound velocity in sediments, pp. 481-518. In: L. Hampton (ed.) Physics of Sound in Marine Sediments. Plenum Press, New York, NY.

Boehme, H., J. F. Byers, T. L. Riley, D. F. Rohde, R. Rolleigh and V.D. Scott. 1980. Environmental Acoustic Measurements for Support of Navy Shallow Water Operations. ARL TR-80-24. Applied Research Laboratories, University of Texas, Austin, TX. 115 pp.

Buchan, S., D. M. McCann and D. T. Smith. 1972. Relations between the acoustic and geotechnical properties of marine sediments. Q. J. Engng. Geol. 5: 265-284.

Bunchuk, A. V. and Yu. Yu. Zhitkovskii. 1981. Sound scattering by the ocean bottom in shallow-water regions (review). Sov. Phy. Acoust. 26: 363-370.

Crisp, J. J., Y. Igarashi and D. R. Jackson. 1980. First Annual Report on TTCP Bottom Scattering Measurements. The Technical Cooperation Program Subgroup G Panel 11. 56 pp.

Folk, R. L. and W. C. Ward. 1957. Brazos River Bar, a study in the significance of grain size parameters. J. Sed. Pet. 27: 3-26.

Hamilton, E. L. 1980. Geoacoustic modeling of the sea floor. J. Acoust. Soc. Am. 68: 1313-1340.

Hamilton, E. L. 1972. Compressional wave attenuation in marine sediments. Geophysics 37: 620-645.

Hamilton, E. L. 1971. Elastic properties of marine sediments. J. Geophys. Res. 76: 579-603.

Hamilton, E. L. and R. T. Bachman. 1982. Sound velocity and related properties of marine sediments. J. Acoust. Soc. Am. 72: 1891-1904.

Hamilton, E. L., H. P. Bucker, D. L. Keir and J. A. Whitney. 1970. Velocities of compressional and shear waves in marine sediments determined in situ from a research submersible. J. Geophys. Res. 75: 4039-4049.

Horn, D. R., B. M. Horn and M. N. Delach. 1968. Correlation between acoustic and other physical properties in deep-sea cores. J. Geophys. Res. 73: 1939-1957.

Mackenzie, K. V. 1981. Nine-term equation for sound speed in the oceans. J. Acoust. Soc. Am. 70: 807-812.

McKinney, C. M. and C. D. Anderson. 1964. Measurement of backscattering of sound from the ocean bottom. J. Acoust. Soc. Am. 36: 158-163.

Nafe, J. E., C. L. Drake. 1963. Physical properties of marine sediments, pp. 794-815. In: M.N. Hill (ed.) The Sea, Vol. 3. Interscience, New York.

NORDA Ocean Programs Office, Code 530. 1982. High Frequency Acoustic Five Year Plan (U). NORDA Technical Note 191 (CONFIDENTIAL).

NSWC. 1982. Mine Warfare Master Plan (U), Naval Surface Weapon Center Working Paper (SECRET).

Richardson, M. D., D. K. Young, K. B. Briggs. 1983. Effects of hydrodynamic and biological processes on sediment geoacoustic properties in Long Island Sound, U.S.A. Mar. Geol. 52:

Richardson, M. D., in press. The effects of bioturbation on sediment elastic properties. Bull. Soc. Geol. France.

APPENDIX A

GRAIN SIZE DISTRIBUTION DATA FOR 11 CORES COLLECTED NEAR THE NOSC OCEANOGRAPHIC TOWER

Grain size data plotted as weight percent histogram and cumulative weight histogram for all phi size through 14ϕ. Also included are percentage gravel, sand, silt, clay, and Folk and Ward (1957) mean phi, standard deviation, skewness, kurtosis and normalized kurtosis.

Station 1

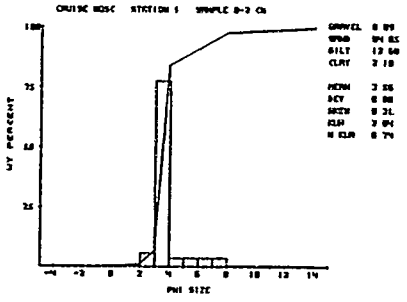

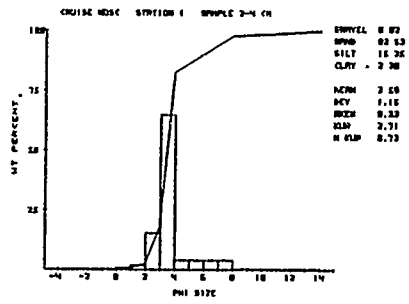

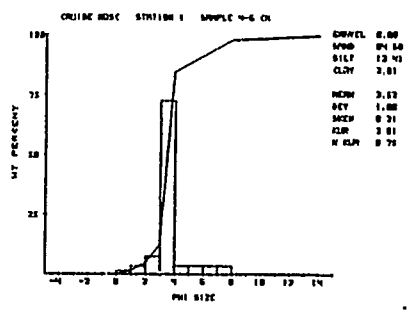

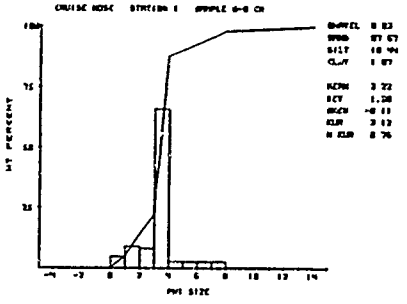

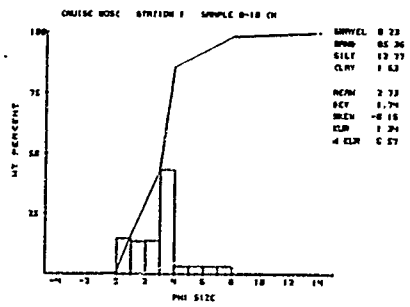

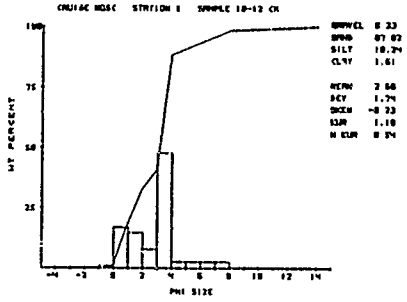

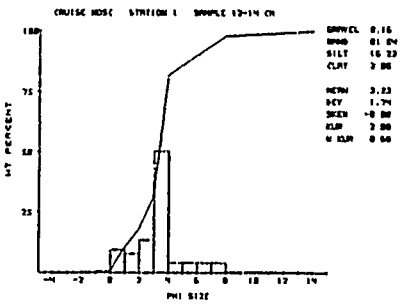

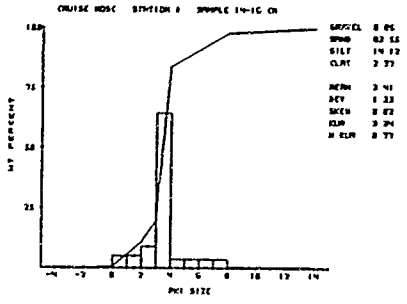

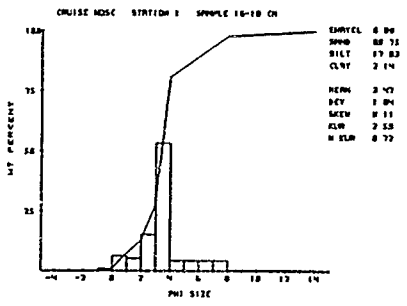

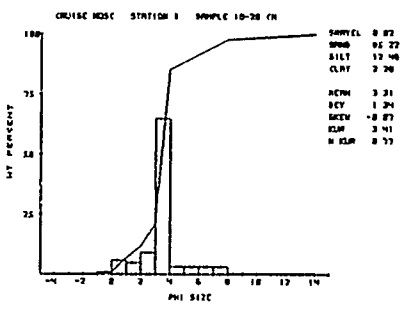

Station 2

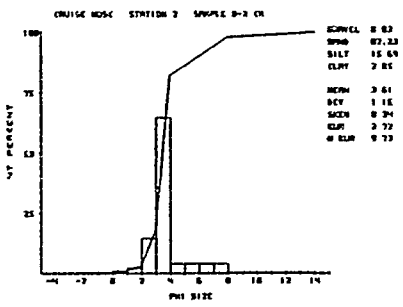

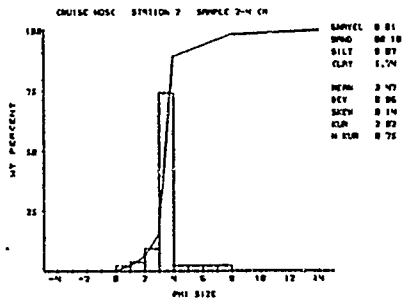

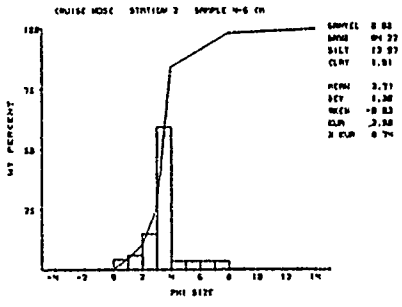

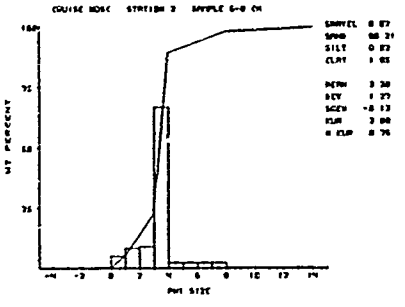

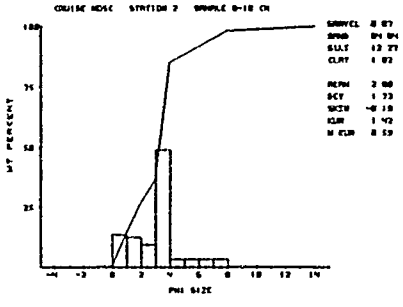

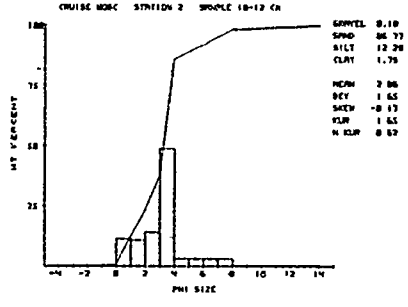

Station 3

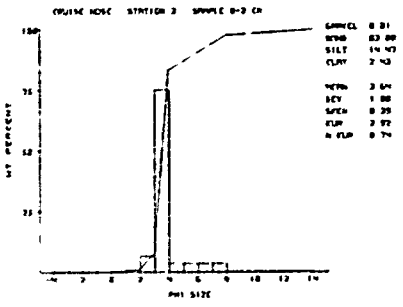

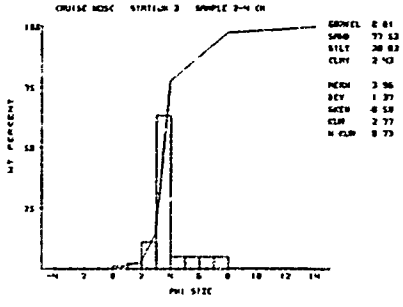

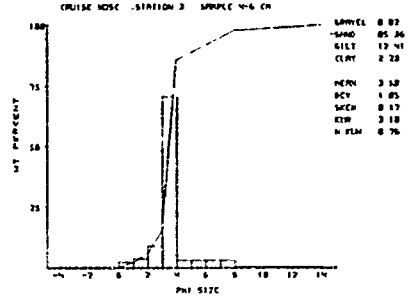

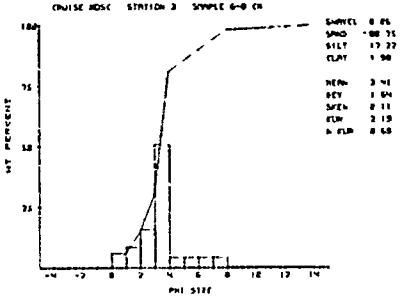

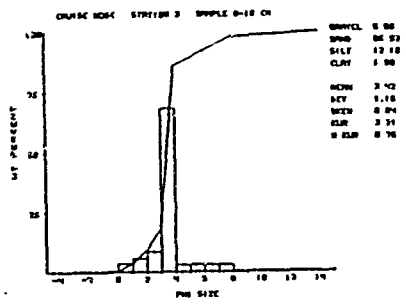

Station 7

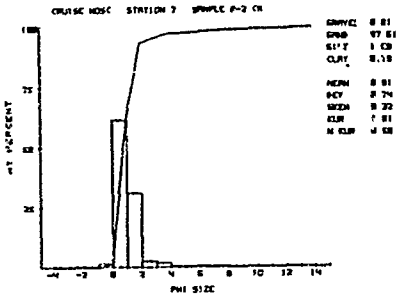

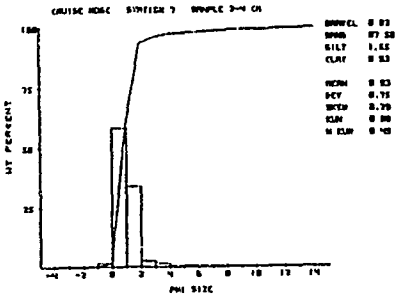

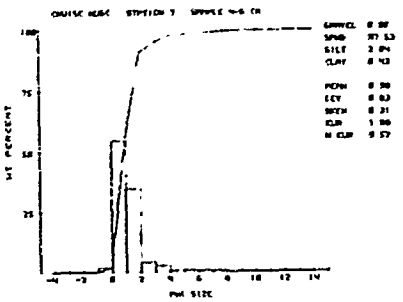

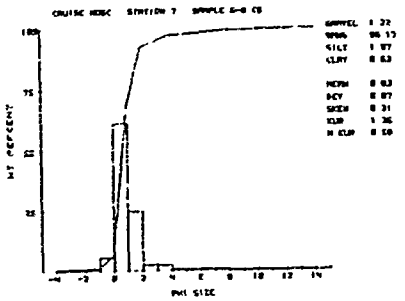

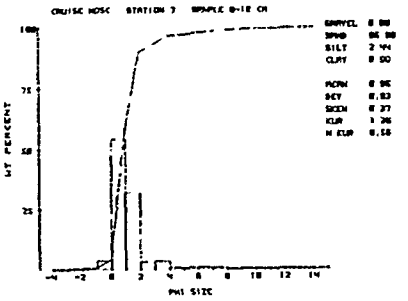

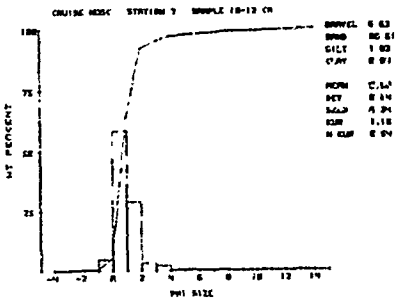

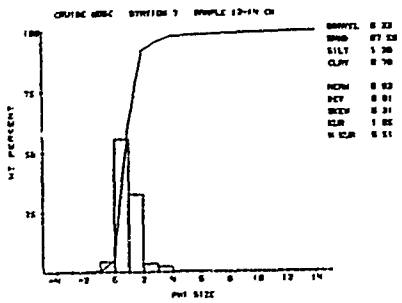

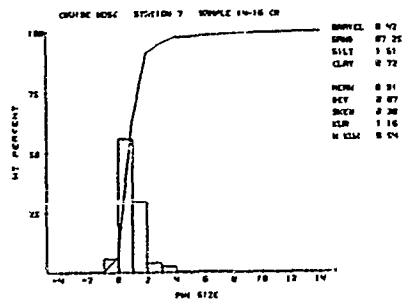

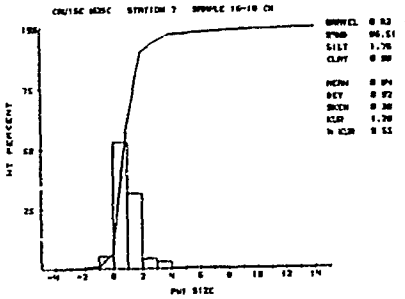

Station 8

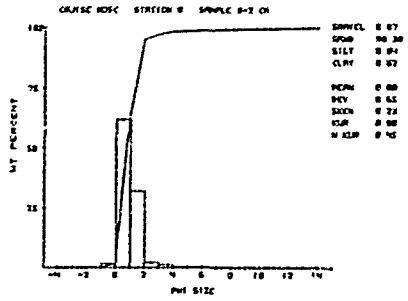

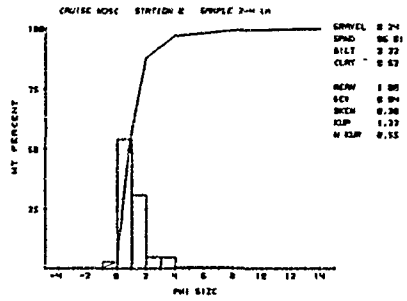

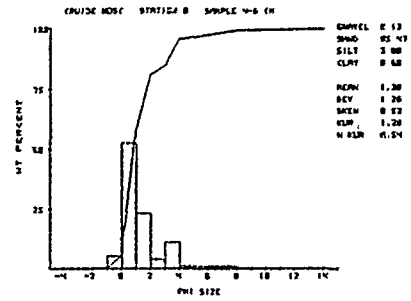

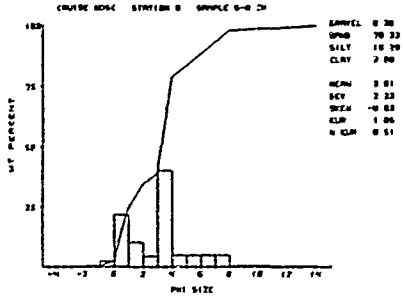

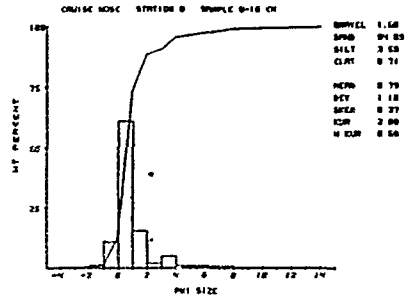

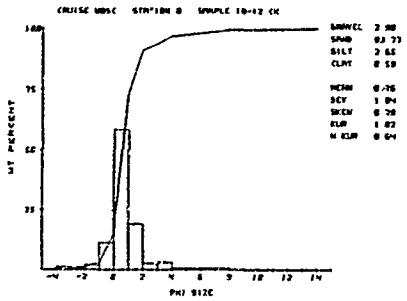

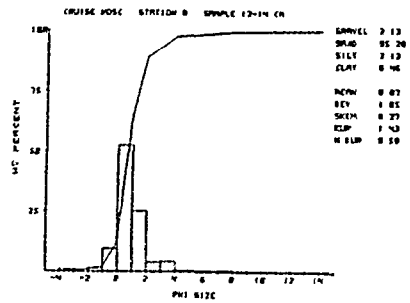

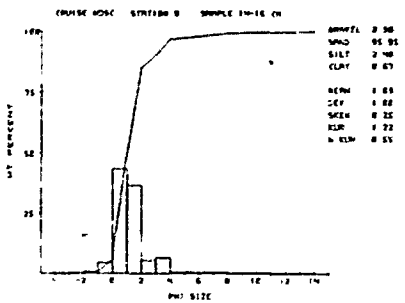

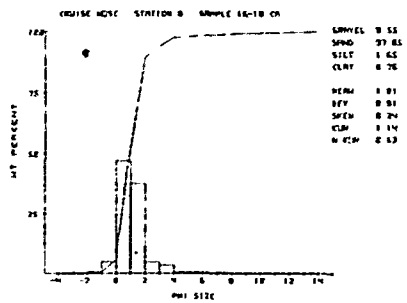

Station 9

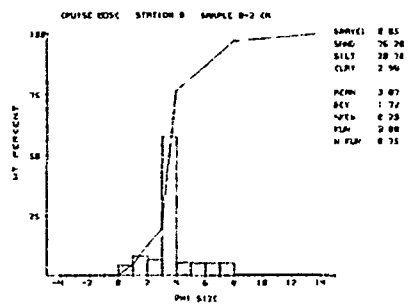

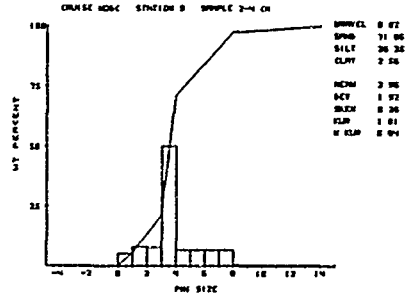

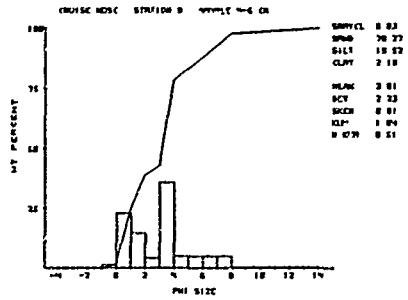

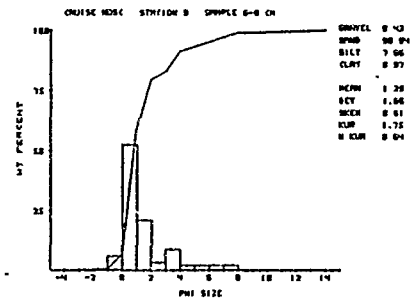

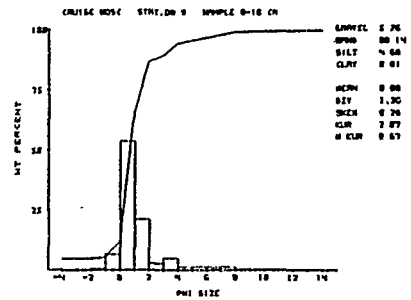

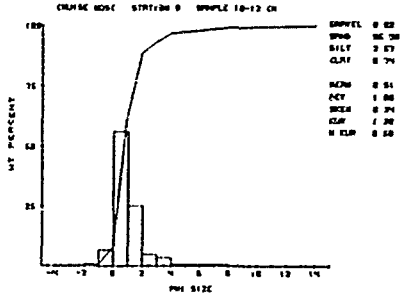

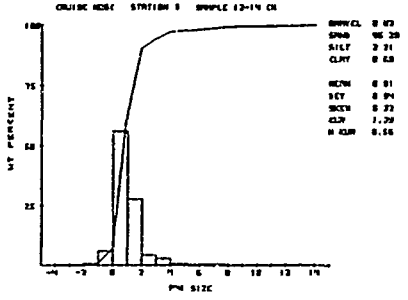

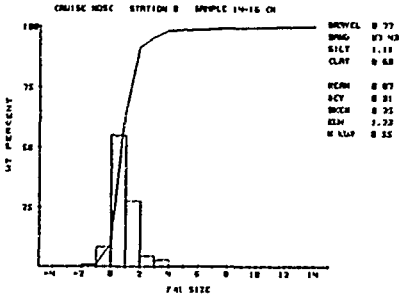

Station 10

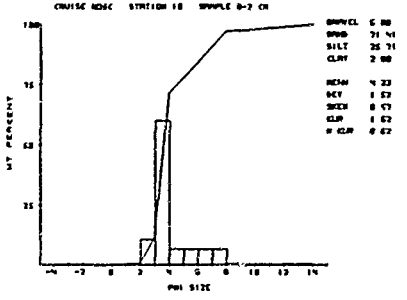

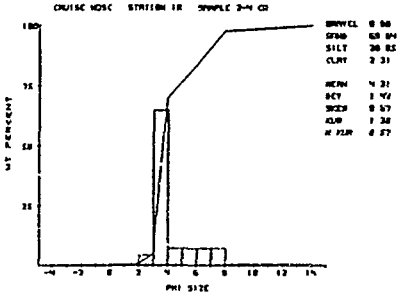

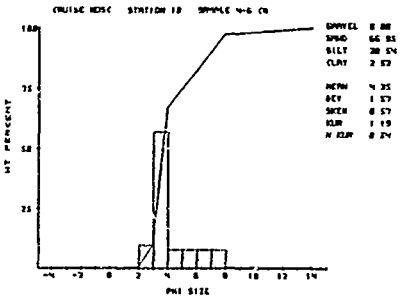

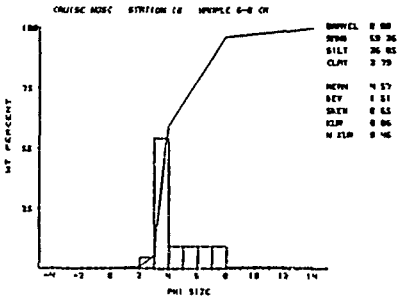

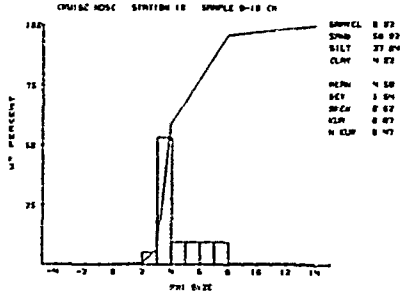

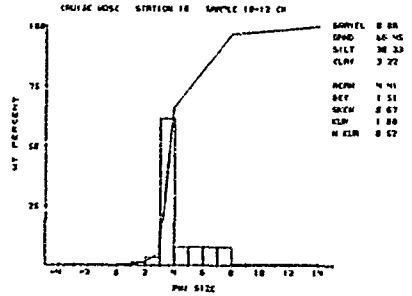

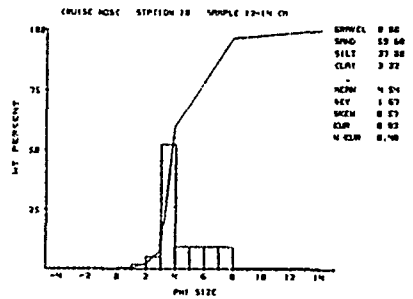

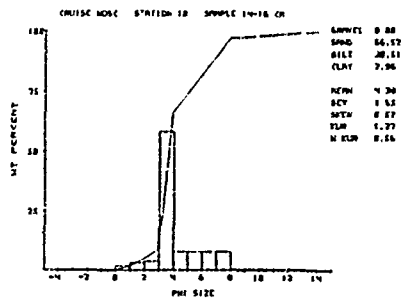

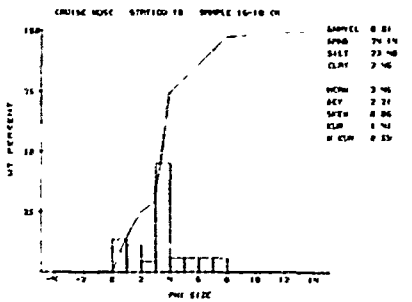

Station 11

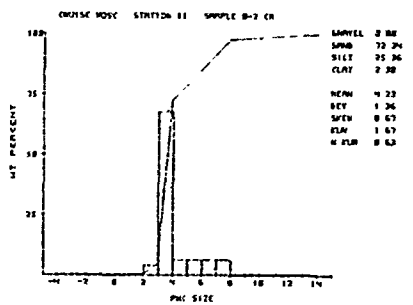

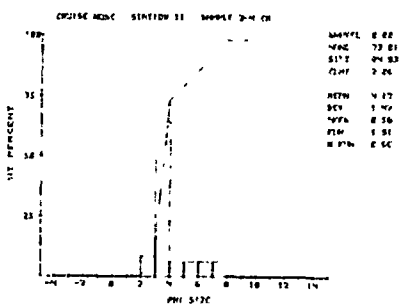

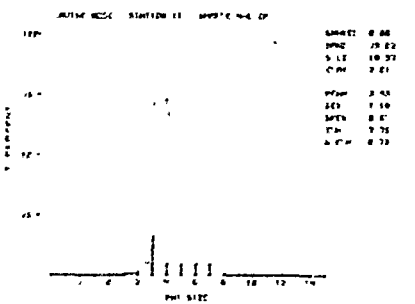

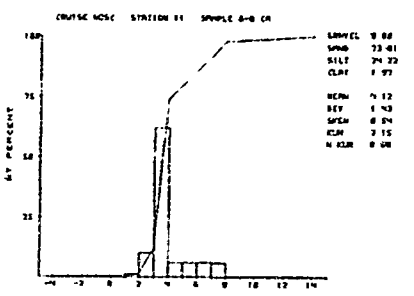

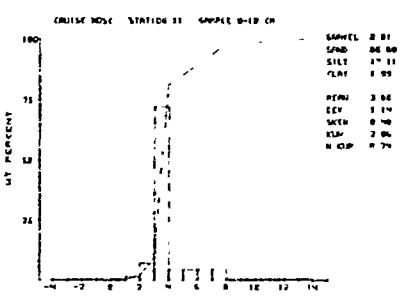

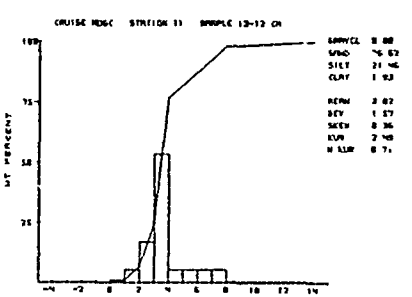

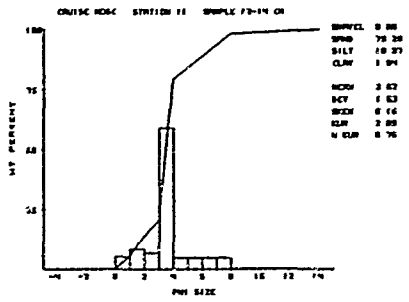

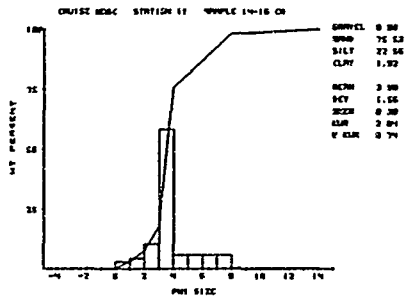

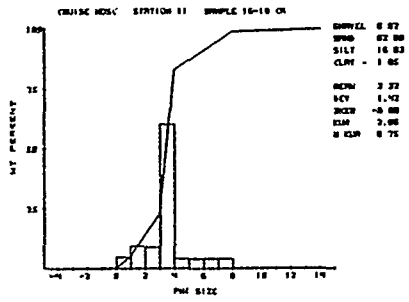

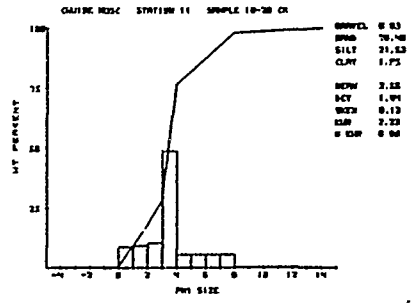

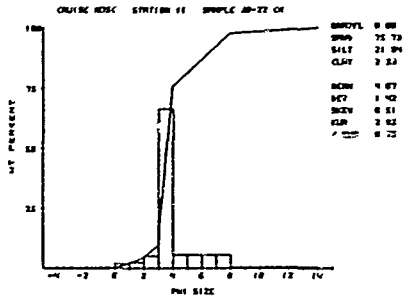

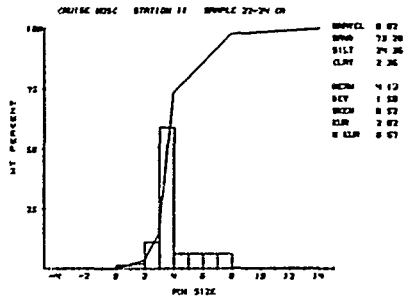

Station 14

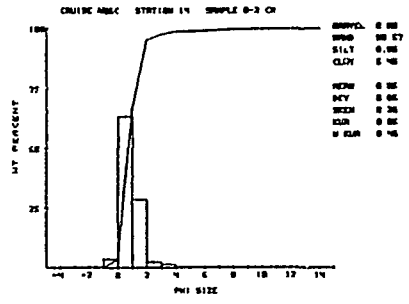

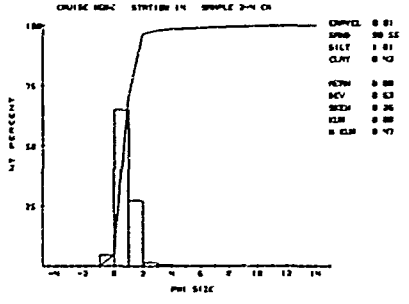

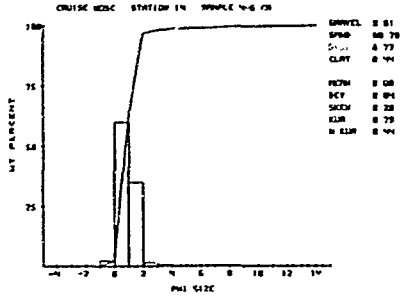

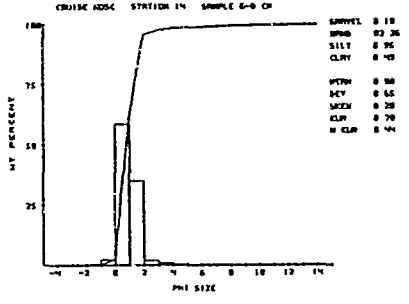

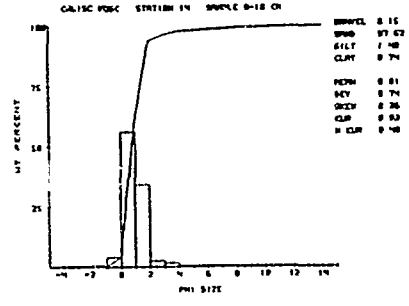

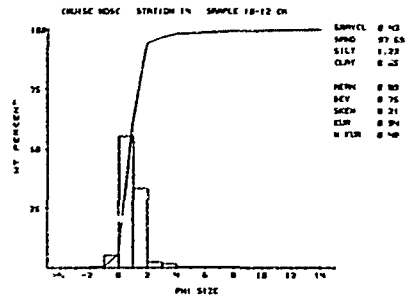

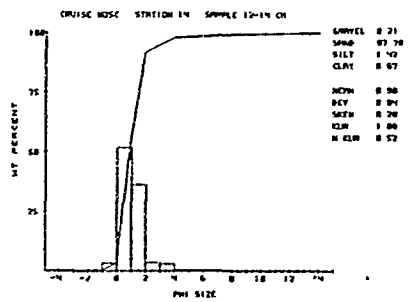

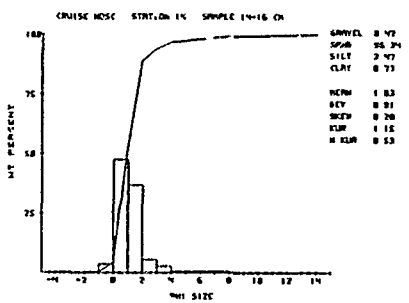

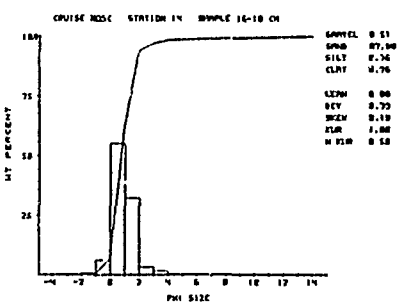

Station 16

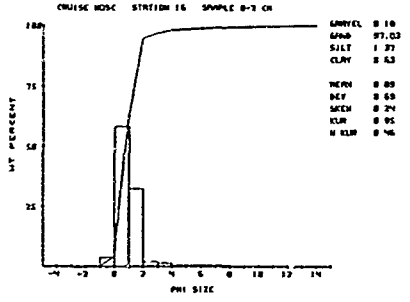

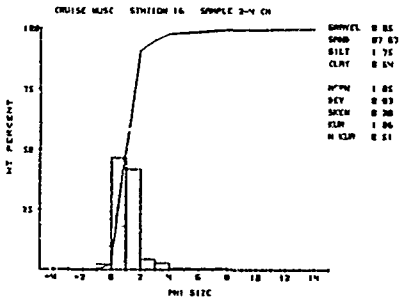

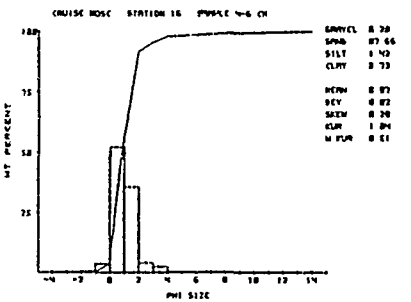

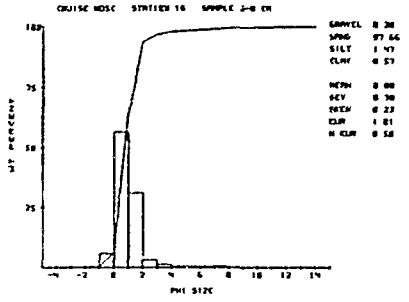

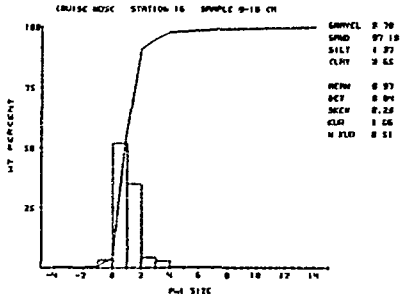

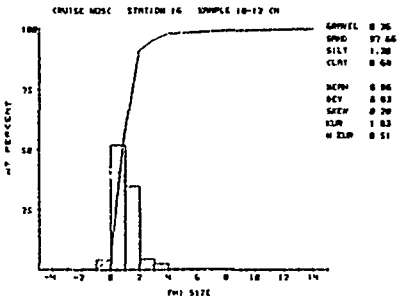

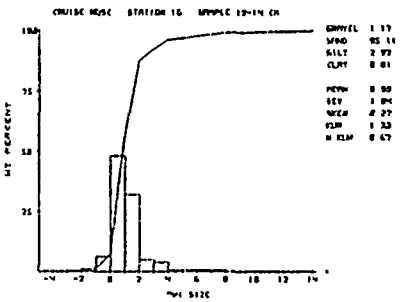

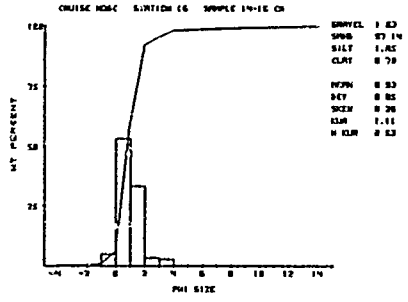

Station 17

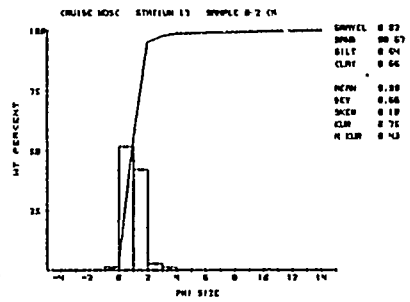

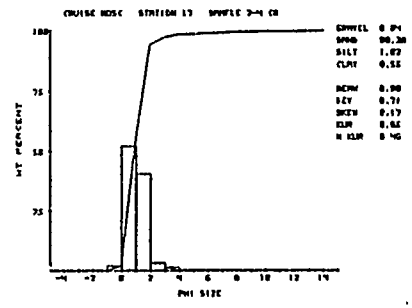

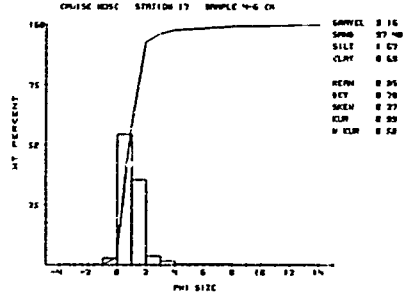

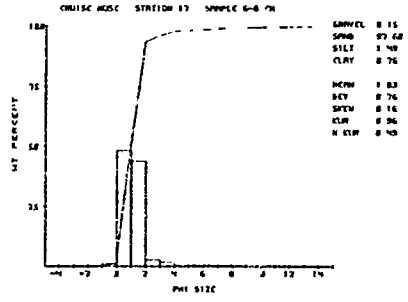

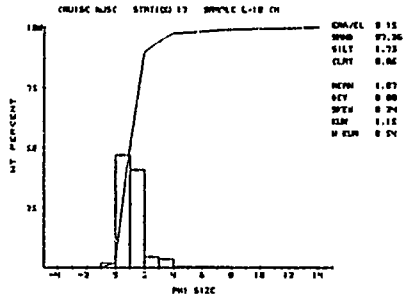

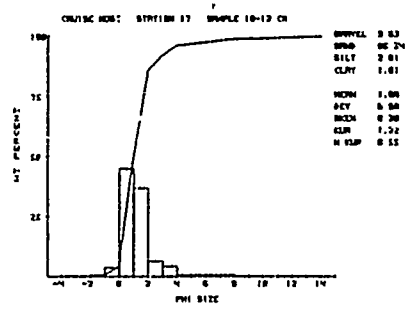

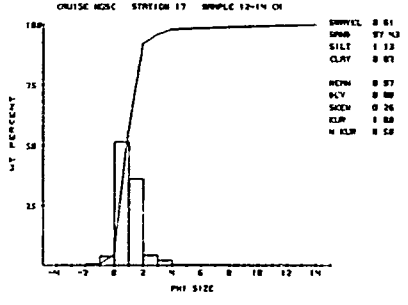

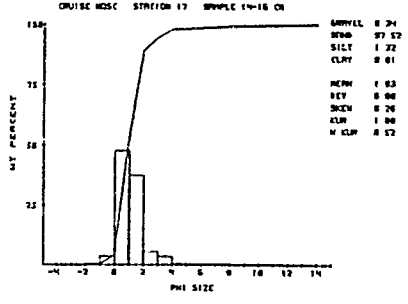

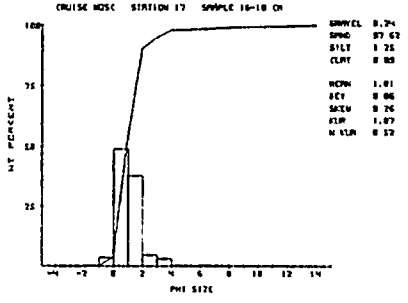

APPENDIX B

COMPRESSIONAL WAVE VELOCITY AND ATTENUATION DATA

Compressional wave velocity (m/sec), velocity ratio, and attenuation expressed as alpha (dB/m) and k for 17 cores collected near the NOSC Oceanographic Tower. Velocities calculated for 23°C, 35 ppt salinity at 0 m depth. Attenuation calculated at 400 kHz.

Cruise: NOSC-TOWER Station: 1 Date: 29 APRIL 1982
Lat: 32-46N Long: 117-16W Depth: 18 m

Calculated for: 23.0 Deg-C 35.00 o/oo 0 m 400 kHz

Depth (cm)	Vp (m/sec)	Vp Ratio	Alpha (dB/m)	k
WATER	1522.5	0.996	0.0	0.000
0.0	1526.0	0.998	27.6	0.069
1.0	1648.1	1.078	174.3	0.436
2.0	1658.4	1.084	174.3	0.436
3.0	1667.0	1.090	168.7	0.422
4.0	1669.3	1.091	163.3	0.408
5.0	1671.1	1.093	174.3	0.436
6.0	1671.1	1.093	168.7	0.422
7.0	1671.6	1.093	168.7	0.422
8.0	1691.9	1.106	180.1	0.450
9.0	1708.5	1.117	180.1	0.450
10.0	1715.2	1.121	229.2	0.573
11.0	1720.5	1.125	206.0	0.515
12.0	1717.1	1.123	221.0	0.553
13.0	1717.1	1.123	267.4	0.668
14.0	1669.7	1.092	256.8	0.642
15.0	1661.1	1.086	180.1	0.450
16.0	1663.8	1.088	192.5	0.481
17.0	1665.6	1.089	192.5	0.481
18.0	1669.3	1.091	206.0	0.515
19.0	1678.4	1.097	291.2	0.728

Cruise: NOSC-TOWER Station: 2 Date: 29 APRIL 1982
Lat: 32-46N Long: 117-16W Depth: 18 m

Calculated for: 23.0 Deg-C 35.00 o/oo 0 m 400 kHz

Depth (cm)	Vp (m/sec)	Vp Ratio	Alpha (dB/m)	k
WATER	1522.2	0.995	4.4	0.011
0.0	1522.2	0.995	4.4	0.011
1.0	1667.5	1.090	233.6	0.584
2.0	1678.7	1.098	153.9	0.385
3.0	1684.7	1.102	159.0	0.398
4.0	1687.5	1.103	159.0	0.398
5.0	1686.1	1.102	153.9	0.385
6.0	1684.3	1.101	164.4	0.411
7.0	1673.7	1.094	153.9	0.385
8.0	1683.3	1.101	188.2	0.471
9.0	1737.4	1.136	399.2	0.998
10.0	1754.4	1.147	323.6	0.809

Cruise: NOSC-TOWER Station: 3 Date: 29 APRIL 1982
Lat: 32-46N Long: 117-16W Depth: 18 m

Calculated for: 23.0 Deg-C 35.00 o/oo 0 m 400 KHz

Depth (cm)	Vp (m/sec)	Vp Ratio	Alpha (dB/m)	k
WATER	1521.2	0.995	0.0	0.000
0.0	1526.9	0.998	53.4	0.133
1.0	1661.5	1.086	160.0	0.400
2.0	1662.9	1.087	149.5	0.374
3.0	1661.1	1.086	139.7	0.349
4.0	1667.4	1.090	149.5	0.374
5.0	1672.9	1.094	160.0	0.400
6.0	1675.2	1.095	149.5	0.374
7.0	1682.1	1.100	160.0	0.400
8.0	1700.9	1.112	204.7	0.512
9.0	1691.5	1.106	220.5	0.551

Cruise: NOSC-TOWER Station: 4 Date: 29 APRIL 1982
Lat: 32-46N Long: 117-16W Depth: 18 m

Calculated for: 23.0 Deg-C 35.00 o/oo 0 m 400 KHz

Depth (cm)	Vp (m/sec)	Vp Ratio	Alpha (dB/m)	k
WATER	1519.3	0.993	8.6	0.022
0.0	1529.2	1.000	107.3	0.268
1.0	1657.9	1.084	180.1	0.450
2.0	1667.4	1.090	163.3	0.408
3.0	1667.0	1.090	163.3	0.408
4.0	1659.3	1.085	163.3	0.408
5.0	1657.9	1.084	158.1	0.395
6.0	1660.6	1.086	168.7	0.422
7.0	1675.2	1.095	206.0	0.515
8.0	1682.6	1.100	192.5	0.481
9.0	1691.9	1.106	247.0	0.617
10.0	1693.3	1.107	319.7	0.799

Cruise: NOSC-TOWER Station: 5 Date: 29 APRIL 1982
Lat: 32-46N Long: 117-16W Depth: 18 m

Calculated for: 23.0 Deg-C 35.00 o/oo 0 m 400 kHz

Depth (cm)	Vp (m/sec)	Vp Ratio	Alpha (dB/m)	k
WATER	1527.9	0.999	0.0	0.000
0.0	1531.0	1.001	8.6	0.022
1.0	1652.8	1.081	180.1	0.450
2.0	1660.0	1.085	163.3	0.408
3.0	1665.8	1.089	168.7	0.422
4.0	1670.9	1.092	174.3	0.436
5.0	1684.2	1.101	180.1	0.450
6.0	1686.5	1.103	180.1	0.450
7.0	1681.4	1.099	174.3	0.436
8.0	1676.4	1.096	180.1	0.450
9.0	1680.5	1.099	180.1	0.450
10.0	1690.3	1.105	206.0	0.515
11.0	1686.1	1.102	199.1	0.498
12.0	1683.3	1.101	206.0	0.515
13.0	1688.9	1.104	206.0	0.515
14.0	1687.9	1.104	192.5	0.481
15.0	1668.1	1.091	206.0	0.515
16.0	1665.4	1.089	192.5	0.481
17.0	1664.9	1.089	192.5	0.481
18.0	1666.7	1.090	186.1	0.465
19.0	1669.5	1.092	186.1	0.465
20.0	1681.4	1.099	213.3	0.533
21.0	1695.9	1.109	256.8	0.642
22.0	1690.3	1.105	221.0	0.553
23.0	1684.2	1.101	206.0	0.515
24.0	1681.0	1.099	247.0	0.617

Cruise: NOSC-TOWER Station: 6 Date: 29 APRIL 1982
Lat: 32-46N Long: 117-16W Depth: 18 m

Calculated for: 23.0 Deg-C 35.00 o/oo 0 m 400 kHz

Depth (cm)	Vp (m/sec)	Vp Ratio	Alpha (dB/m)	k
WATER	1526.9	0.998	-8.6	-0.022
0.0	1532.3	1.002	29.6	0.074
1.0	1659.5	1.085	183.8	0.460
2.0	1667.7	1.090	154.7	0.387
3.0	1666.8	1.090	154.7	0.387
4.0	1661.3	1.086	160.0	0.400
5.0	1680.0	1.099	197.4	0.493
6.0	1685.1	1.102	160.0	0.400
7.0	1679.1	1.098	160.0	0.400
8.0	1678.0	1.097	160.0	0.400
9.0	1676.1	1.096	160.0	0.400
10.0	1674.8	1.095	149.5	0.374
11.0	1675.2	1.095	171.4	0.429
12.0	1672.5	1.094	183.8	0.460
13.0	1666.6	1.090	171.4	0.429
14.0	1666.6	1.090	171.4	0.429
15.0	1664.7	1.089	171.4	0.429
16.0	1662.0	1.087	171.4	0.429
17.0	1661.1	1.086	171.4	0.429
18.0	1658.4	1.084	229.2	0.573
19.0	1667.5	1.090	229.2	0.573
20.0	1669.7	1.092	229.2	0.573
21.0	1669.7	1.092	197.4	0.493
22.0	1671.1	1.093	204.7	0.512
23.0	1674.3	1.095	183.8	0.460
24.0	1673.9	1.094	183.8	0.460

Cruise: NOSC-TOWER Station: 7 Date: 4 MAY 1982
Lat: 32-46N Long: 117-16W Depth: 18 m

Calculated for: 23.0 Deg-C 35.00 o/oo 0 m 400 kHz

Depth (cm)	Vp (m/sec)	Vp Ratio	Alpha (dB/m)	k
WATER	1526.1	0.998	4.1	0.010
0.0	1529.9	1.000	66.1	0.165
1.0	1738.2	1.137	152.4	0.381
2.0	1740.5	1.138	72.7	0.182
3.0	1749.9	1.144	72.7	0.182
4.0	1751.8	1.145	72.7	0.182
5.0	1745.4	1.141	66.1	0.165
6.0	1753.8	1.147	102.8	0.257
7.0	1739.5	1.137	203.2	0.508
8.0	1716.3	1.122	203.2	0.508
9.0	1700.3	1.112	233.3	0.583
10.0	1699.8	1.111	251.1	0.628
11.0	1754.8	1.147	167.4	0.419
12.0	1761.8	1.152	111.5	0.279
13.0	1764.3	1.154	111.5	0.279
14.0	1769.9	1.157	111.5	0.279
15.0	1770.9	1.158	120.6	0.302
16.0	1773.0	1.159	141.0	0.353
17.0	1770.9	1.158	141.0	0.353

Cruise: NOSC-TOWER Station: 8 Date: 4 MAY 1982
Lat: 32-46N Long: 117-16W Depth: 18 m

Calculated for: 23.0 Deg-C 35.00 o/oo 0 m 400 kHz

Depth (cm)	Vp (m/sec)	Vp Ratio	Alpha (dB/m)	k
WATER	1527.7	0.999	0.0	0.000
0.0	1631.3	1.067	178.4	0.446
1.0	1738.7	1.137	79.7	0.199
2.0	1757.8	1.149	102.8	0.257
3.0	1764.3	1.154	94.7	0.237
4.0	1784.7	1.167	130.5	0.326
5.0	1798.2	1.176	143.2	0.358
6.0	1796.1	1.174	282.9	0.707
7.0	1660.1	1.085	241.9	0.605
8.0	1684.5	1.101	492.7	1.232
9.0	1764.3	1.154	233.3	0.583
10.0	1756.8	1.149	152.4	0.381
11.0	1748.4	1.143	172.8	0.432
12.0	1753.3	1.146	210.2	0.525
13.0	1756.8	1.149	203.2	0.508
14.0	1759.8	1.151	225.2	0.563
15.0	1768.9	1.157	172.8	0.432
16.0	1772.4	1.159	172.8	0.432
17.0	1777.0	1.162	178.4	0.446
18.0	1774.0	1.160	172.8	0.432

Cruise: NOSC-TOWER Station: 9 Date: 4 MAY 1982
Lat: 32-46N Long: 117-16W Depth: 18 m

Calculated for: 23.0 Deg-C 35.00 o/oo 0 m 400 kHz

Depth (cm)	Vp (m/sec)	Vp Ratio	Alpha (dB/m)	k
WATER	1525.6	0.998	-4.0	-0.010
0.0	1532.1	1.002	47.9	0.120
1.0	1639.1	1.072	210.2	0.525
2.0	1648.3	1.078	210.2	0.525
3.0	1665.7	1.089	210.2	0.525
4.0	1657.2	1.084	225.2	0.563
5.0	1660.7	1.086	251.1	0.628
6.0	1714.7	1.121	332.0	0.830
7.0	1746.3	1.142	251.1	0.628
8.0	1776.4	1.162	178.4	0.446
9.0	1781.0	1.165	126.5	0.316
10.0	1773.3	1.160	241.9	0.605
11.0	1782.6	1.166	282.9	0.707
12.0	1775.9	1.161	152.4	0.381
13.0	1764.7	1.154	130.5	0.326
14.0	1764.7	1.154	120.6	0.302
15.0	1764.7	1.154	130.5	0.326
16.0	1767.8	1.156	130.5	0.326

Cruise: NOSC-TOWER Station: 10 Date: 4 MAY 1982
Lat: 32-46N Long: 117-16W Depth: 18 m

Calculated for: 23.0 Deg-C 35.00 o/oo 0 m 400 kHz

Depth (cm)	Vp (m/sec)	Vp Ratio	Alpha (dB/m)	k
WATER	1526.8	0.998	4.1	0.010
0.0	1530.2	1.001	26.8	0.067
1.0	1629.1	1.065	225.2	0.563
2.0	1643.1	1.074	203.2	0.508
3.0	1654.1	1.082	184.2	0.460
4.0	1645.7	1.076	162.2	0.406
5.0	1651.4	1.080	162.2	0.406
6.0	1653.6	1.081	162.2	0.406
7.0	1650.1	1.079	178.4	0.446
8.0	1630.5	1.066	241.9	0.605
9.0	1612.6	1.054	172.8	0.432
10.0	1617.2	1.057	167.4	0.419
11.0	1623.2	1.061	162.2	0.406
12.0	1626.2	1.063	167.4	0.419
13.0	1622.3	1.061	167.4	0.419
14.0	1620.2	1.059	167.4	0.419
15.0	1626.6	1.064	178.4	0.446
16.0	1632.2	1.067	178.4	0.446

Cruise: NOSC-TOWER Station: 11 Date: 5 MAY 1982
Lat: 32-46N Long: 117-16W Depth: 18 m

Calculated for: 23.0 Deg-C 35.00 o/oo 0 m 400 kHz

Depth (cm)	Vp (m/sec)	Vp Ratio	Alpha (dB/m)	k
WATER	1525.7	0.998	0.0	0.000
0.0	1531.8	1.002	59.8	0.149
1.0	1646.9	1.077	196.6	0.491
2.0	1665.5	1.089	172.8	0.432
3.0	1669.6	1.092	152.4	0.381
4.0	1670.5	1.092	157.2	0.393
5.0	1674.2	1.095	162.2	0.406
6.0	1671.9	1.093	167.4	0.419
7.0	1669.1	1.091	162.2	0.406
8.0	1676.5	1.096	184.2	0.460
9.0	1684.3	1.101	178.4	0.446
10.0	1682.0	1.100	162.2	0.406
11.0	1687.5	1.103	167.4	0.419
12.0	1688.9	1.104	172.8	0.432
13.0	1696.9	1.110	184.2	0.460
14.0	1701.6	1.113	196.6	0.491
15.0	1701.1	1.112	217.5	0.544
16.0	1680.1	1.099	172.8	0.432
17.0	1686.6	1.103	190.3	0.476
18.0	1705.4	1.115	225.2	0.563
19.0	1703.0	1.114	241.9	0.605
20.0	1692.7	1.107	241.9	0.605
21.0	1692.7	1.107	225.2	0.563
22.0	1708.2	1.117	271.5	0.679
23.0	1700.6	1.112	251.1	0.628

Cruise: NOSC-TOWER Station: 12 Date: 5 MAY 1982
Lat: 32-46N Long: 117-16W Depth: 18 m

Calculated for: 23.0 Deg-C 35.00 o/oo 0 m 400 kHz

Depth (cm)	Vp (m/sec)	Vp Ratio	Alpha (dB/m)	k
WATER	1524.9	0.997	0.0	0.000
0.0	1530.2	1.001	31.8	0.079
1.0	1654.9	1.082	203.2	0.508
2.0	1668.9	1.091	172.8	0.432
3.0	1671.6	1.093	167.4	0.419
4.0	1668.0	1.091	167.4	0.419
5.0	1669.8	1.092	178.4	0.446
6.0	1673.5	1.094	172.8	0.432
7.0	1677.6	1.097	167.4	0.419
8.0	1680.3	1.099	172.8	0.432
9.0	1682.7	1.100	167.4	0.419
10.0	1691.5	1.106	196.6	0.491
11.0	1697.6	1.110	196.6	0.491
12.0	1702.3	1.113	233.3	0.583
13.0	1771.6	1.158	407.6	1.019
14.0	1779.3	1.163	241.9	0.605
15.0	1698.0	1.110	480.3	1.201
16.0	1691.0	1.106	196.6	0.491
17.0	1693.3	1.107	225.2	0.563
18.0	1692.4	1.107	225.2	0.563
19.0	1686.4	1.103	225.2	0.563
20.0	1679.4	1.098	203.2	0.508
21.0	1682.2	1.100	210.2	0.525
22.0	1677.1	1.097	203.2	0.508
23.0	1669.8	1.092	190.3	0.476

Cruise: NOSC-TOWER Station: 13 Date: 5 MAY 1982
Lat: 32-46N Long: 117-16W Depth: 18 m

Calculated for: 23.0 Deg-C 35.00 o/oo 0 m 400 kHz

Depth (cm)	Vp (m/sec)	Vp Ratio	Alpha (dB/m)	k
WATER	1523.2	0.996	0.0	0.000
0.0	1550.1	1.014	193.4	0.483
1.0	1671.0	1.093	167.4	0.419
2.0	1670.3	1.092	152.4	0.381
3.0	1670.7	1.092	157.2	0.393
4.0	1669.8	1.092	167.4	0.419
5.0	1668.5	1.091	162.2	0.406
6.0	1671.7	1.093	167.4	0.419
7.0	1673.0	1.094	162.2	0.406
8.0	1676.7	1.096	190.3	0.476
9.0	1667.1	1.090	172.8	0.432
10.0	1669.4	1.092	184.2	0.460
11.0	1673.0	1.094	225.2	0.563
12.0	1666.2	1.089	217.5	0.544
13.0	1662.1	1.087	190.3	0.476
14.0	1666.7	1.090	196.6	0.491

Cruise: NOSC-TOWER Station: 14 Date: 5 MAY 1982
Lat: 32-46N Long: 117-16W Depth: 18 m

Calculated for: 23.0 Deg-C 35.00 o/oo 0 m 400 kHz

Depth (cm)	Vp (m/sec)	Vp Ratio	Alpha (dB/m)	k
WATER	1524.6	0.997	4.3	0.011
0.0	1627.2	1.064	186.1	0.465
1.0	1726.3	1.129	98.7	0.247
2.0	1728.5	1.130	82.9	0.207
3.0	1726.1	1.129	75.6	0.189
4.0	1725.6	1.128	75.6	0.189
5.0	1733.4	1.133	75.6	0.189
6.0	1741.8	1.139	90.6	0.226
7.0	1745.8	1.141	98.7	0.247
8.0	1746.3	1.142	107.3	0.268
9.0	1747.3	1.142	107.3	0.268
10.0	1746.3	1.142	126.3	0.316
11.0	1739.3	1.137	116.5	0.291
12.0	1745.8	1.141	139.1	0.348
13.0	1748.8	1.143	107.3	0.268
14.0	1752.8	1.146	116.5	0.291
15.0	1760.3	1.151	126.3	0.316
16.0	1760.3	1.151	126.3	0.316
17.0	1765.4	1.154	126.3	0.316
18.0	1768.0	1.156	148.3	0.371
19.0	1758.8	1.150	148.3	0.371

Cruise: NOSC-TOWER Station: 15 Date: 5 MAY 1982
Lat: 32-46N Long: 117-16W Depth: 18 m

Calculated for: 23.0 Deg-C 35.00 o/oo 0 m 400 kHz

Depth (cm)	Vp (m/sec)	Vp Ratio	Alpha (dB/m)	k
WATER	2032.9	1.329	17.8	0.045
0.0	1526.7	0.998	62.0	0.155
1.0	1725.6	1.128	213.3	0.533
2.0	1731.7	1.132	116.5	0.291
3.0	1739.6	1.137	82.9	0.207
4.0	1741.6	1.139	90.6	0.226
5.0	1744.6	1.141	90.6	0.226
6.0	1744.6	1.141	90.6	0.226
7.0	1741.6	1.139	107.3	0.268
8.0	1739.1	1.137	107.3	0.268
9.0	1741.1	1.138	98.7	0.247
10.0	1740.1	1.138	126.3	0.316
11.0	1746.5	1.142	134.7	0.337
12.0	1748.0	1.143	153.1	0.383
13.0	1749.0	1.144	114.6	0.287
14.0	1759.1	1.150	126.3	0.316
15.0	1771.3	1.158	143.6	0.359
16.0	1770.3	1.158	139.1	0.348
17.0	1775.4	1.161	192.5	0.481

Cruise: NOSC-TOWER Station: 16 Date: 5 MAY 1982
Lat: 32-46N Long: 117-16W Depth: 18 m

Calculated for: 23.0 Deg-C 35.00 o/oo 0 m 400 kHz

Depth (cm)	Vp (m/sec)	Vp Ratio	Alpha (dB/m)	k
WATER	1522.7	0.996	0.0	0.000
0.0	1743.0	1.140	225.0	0.563
1.0	1743.0	1.140	98.7	0.247
2.0	1744.6	1.141	68.6	0.172
3.0	1759.6	1.151	98.7	0.247
4.0	1774.4	1.160	82.9	0.207
5.0	1777.0	1.162	107.3	0.268
6.0	1768.8	1.157	98.7	0.247
7.0	1768.8	1.157	98.7	0.247
8.0	1768.8	1.157	107.3	0.268
9.0	1771.8	1.159	116.5	0.291
10.0	1773.4	1.160	126.3	0.316
11.0	1771.3	1.158	116.5	0.291
12.0	1774.9	1.161	126.3	0.316
13.0	1778.0	1.163	126.3	0.316
14.0	1773.9	1.160	126.3	0.316
15.0	1769.3	1.157	174.3	0.436

Cruise: NOSC-TOWER Station: 17 Date: 5 MAY 1982
Lat: 32-46N Long: 117-16W Depth: 18 m

Calculated for: 23.0 Deg-C 35.00 o/oo 0 m 400 kHz

Depth (cm)	Vp (m/sec)	Vp Ratio	Alpha (dB/m)	k
WATER	1523.1	0.996	12.8	0.032
0.0	1752.0	1.146	178.4	0.446
1.0	1743.0	1.140	79.7	0.199
2.0	1740.1	1.138	59.8	0.149
3.0	1740.6	1.138	72.7	0.182
4.0	1745.0	1.141	79.7	0.199
5.0	1745.0	1.141	79.7	0.199
6.0	1748.5	1.143	87.0	0.217
7.0	1756.6	1.149	94.7	0.237
8.0	1757.6	1.149	87.0	0.217
9.0	1769.8	1.157	120.6	0.302
10.0	1767.2	1.156	111.5	0.279
11.0	1771.8	1.159	120.6	0.302
12.0	1767.7	1.156	130.5	0.326
13.0	1778.0	1.163	143.2	0.358
14.0	1779.6	1.164	152.4	0.381
15.0	1782.7	1.166	147.8	0.369
16.0	1793.1	1.172	157.2	0.393
17.0	1790.0	1.170	152.4	0.381
18.0	1783.2	1.166	143.2	0.358

UNCLASSIFIED

SECURITY CLASSIFICATION OF THIS PAGE *(When Data Entered)*

REPORT DOCUMENTATION PAGE		READ INSTRUCTIONS BEFORE COMPLETING FORM
1. REPORT NUMBER NORDA Technical Note 219	2. GOVT ACCESSION NO. AD-B076	3. RECIPIENT'S CATALOG NUMBER 818L
4. TITLE *(and Subtitle)* Environmental Support for High Frequency Acoustic Measurements at NOSC Oceanographic Tower, 26 April - 7 May 1982; Part I: Sediment Geoacoustic Properties		5. TYPE OF REPORT & PERIOD COVERED Final 6. PERFORMING ORG. REPORT NUMBER
7. AUTHOR(s) Michael D. Richardson David K. Young Richard I. Ray		8. CONTRACT OR GRANT NUMBER(s)
9. PERFORMING ORGANIZATION NAME AND ADDRESS		10 PROGRAM ELEMENT, PROJECT, TASK AREA & WORK UNIT NUMBERS 62759N
11. CONTROLLING OFFICE NAME AND ADDRESS		12. REPORT DATE June 1983 13. NUMBER OF PAGES 68
14. MONITORING AGENCY NAME & ADDRESS*(if different from Controlling Office)*		15. SECURITY CLASS. *(of this report)* UNCLASSIFIED 15a. DECLASSIFICATION/DOWNGRADING SCHEDULE

16. DISTRIBUTION STATEMENT *(of this Report)*

~~Approved for Public Release~~
~~Distribution Unlimited~~

17. DISTRIBUTION STATEMENT *(of the abstract entered in Block 20, if different from Report)*

18. SUPPLEMENTARY NOTES

19. KEY WORDS *(Continue on reverse side if necessary and identify by block number)*

geoacoustic models
high frequency acoustics
mine-hunting sonar
environmental acoustic models

20. ABSTRACT *(Continue on reverse side if necessary and identify by block number)*

This is the first of a four-volume report on environmental support for a joint University of Texas Applied Research Laboratory (UT-ARL)-Naval Ocean Research and Development Activity (NORDA) high frequency acoustic experiment. The experiment was conducted near the Naval Ocean Systems Center (NOSC) Oceano graphic Tower, one mile off the California coast near San Diego, California, from 26 April to 7 May 1982. The objective was to provide improved shallow-water acoustic models required for development of advanced mine hunting sonar systems.

(continued)

DD FORM 1 JAN 73 1473 EDITION OF 1 NOV 65 IS OBSOLETE
S/N 0102-LF-014-6601

UNCLASSIFIED
SECURITY CLASSIFICATION OF THIS PAGE *(When Data Entered)*

(continued from Block 20)

In this report, we present sediment geoacoustic measurements made currently with backscatter measurements for the NOSC Tower Experiment.

Two sediment types were evident from visual (SCUBA) observation and from laboratory analysis of sediment geoacoustic properties. The sediments closest to the transmit-receive tripod were coarse sands with higher compressional wave velocity and lower attenuation and impedence values than those of fine sands surrounding the target spheres.

	Sediment Type	
Geoacoustic Property	Coarse Sand	Fine Sand
Mean Grain Size	0.96	3.53
Velocity Ration	1.15	1.10
Attenuation (k)	0.29	0.47
Compressional Wave Velocity (m/sec) @ 15°C, 34 ppt, 18m	1730	1655
Sediment Impedance (g/cm^2 sec $\cdot$ 10^5) @ 15°C, 34 ppt, 18m	0.322	0.366

Sediment compressional wave velocity and attenuation increased with depth in the sediment, probably as a result of a decrease in porosity due to compaction and packing. The differences between measured and predicted sediment acoustic properties can be explained by these gradients in geoacoustic properties. Historical data from near the NOSC Oceanographic Tower support these conclusions.

These surfical gradients in sediment geoacoustic properties may be important factors in the prediction of high frequency bottom reverberation.